https://doi.org/10.1093/plphys/kiac178 PLANT PHYSIOLOGY 2022: 189: 1608–1624

Plant Physiology®

Research Article

The rice transcription factor Nhd1 regulates root growth and nitrogen uptake by activating nitrogen transporters

Kangning Li ,[1] Shunan Zhang ,[1,*,†] Shuo Tang ,[1] Jun Zhang,[1] Hongzhang Dong ,[1] Shihan Yang ,[1] Hongye Qu,[1] Wei Xuan ,[1] Mian Gu [1] and Guohua Xu [1,*,†]

1 State Key Laboratory of Crop Genetics and Germplasm Enhancement, Key Laboratory of Plant Nutrition and Fertilization in Low-Middle Reaches of the Yangtze River, Ministry of Agriculture, Nanjing Agricultural University, Nanjing 210095, China

*Authors for correspondence: zhangsn@njau.edu.cn (S.Z.); ghxu@njau.edu.cn (G.X.)
†Senior authors.

S.Z., G.X., and K.L. planned and designed the research. K.L., S.Z., and S.T. conducted most of the experiments and data analysis. M.G. conducted the immunostaining analysis. J.Z., H.D., Y. S., and H.Q. contributed to experimental analysis. G.X., S.Z., and K.L. wrote the manuscript.
The author responsible for distribution of materials integral to the findings presented in this article in accordance with the policy described in the Instructions for Authors (https://academic.oup.com/plphys/pages/general-instructions) is: Guohua Xu (ghxu@njau.edu.cn).

Abstract

Plants adjust root architecture and nitrogen (N) transporter activity to meet the variable N demand, but their integrated regulatory mechanism remains unclear. We have previously reported that a floral factor in rice (*Oryza sativa*), N-mediated heading date-1 (Nhd1), regulates flowering time. Here, we show that Nhd1 can directly activate the transcription of the high-affinity ammonium (NH_4^+) transporter 1;3 (*OsAMT1;3*) and the dual affinity nitrate (NO_3^-) transporter 2.4 (*OsNRT2.4*). Knockout of *Nhd1* inhibited root growth in the presence of NO_3^- or a low concentration of NH_4^+. Compared to the wild-type (WT), *nhd1* and *osamt1;3* mutants showed a similar decrease in root growth and N uptake under low NH_4^+ supply, while *nhd1* and *osnrt2.4* mutants showed comparable root inhibition and altered NO_3^- translocation in shoots. The defects of *nhd1* mutants in NH_4^+ uptake and root growth response to various N supplies were restored by overexpression of *OsAMT1;3* or *OsNRT2.4*. However, when grown in a paddy field with low N availability, *nhd1* mutants accumulated more N and achieved a higher N uptake efficiency (NUpE) due to the delayed flowering time and prolonged growth period. Our findings reveal a molecular mechanism underlying the growth duration-dependent NUpE.

Introduction

Ammonium (NH_4^+) and nitrate (NO_3^-) are the major inorganic nitrogen (N) sources acquired by plant roots from soil (Miller and Cramer, 2004; Xu et al., 2012). In flooded soil, NH_4^+ is the dominant N form, since nitrification is inhibited in such condition (Wang et al., 1993; Kronzucker et al., 2000). Rice (*Oryza sativa*) can transport and secrete oxygen generated from shoot photosynthesis to the rhizosphere through its well-developed aerenchyma where oxygen can stimulate the proliferation and growth of nitrifying bacteria (Briones Jr et al., 2003). With the action of nitrifying bacteria, a part of NH_4^+ can be converted into NO_3^- through nitrification process (Li et al., 2008). Paddy rice generally grows under flooded soil in early stage, while it undergoes alternative drying and wetting management of soil in later stage (Bouman and Tuong, 2001; Belder et al., 2004). Therefore, paddy rice at the late growth stage can absorb NO_3^- in large quantity (Arth et al., 1998; Kirk and Kronzucker, 2005).

Received March 02, 2022. Accepted March 21, 2022. Advance access publication April 20, 2022

Many transporter genes belonging to ammonium transporter (AMT) family have been demonstrated to contribute to root NH_4^+ acquisition (Loque and von Wiren, 2004; Li et al., 2012; Tegeder and Masclaux-Daubresse, 2018). Rice genome contains at least 10 AMT genes (Sonoda et al., 2003; Ferreira et al., 2015). OsAMT1;1 contributes ~25% of the total NH_4^+ uptake capacity in roots at both low and high concentration ranges (Li et al., 2016). Triple knockout of *OsAMT1;1*, *OsAMT1;2*, and *OsAMT1;3* resulted in ~95% reduction of NH_4^+ uptake (Konishi and Ma, 2021), suggesting AMTs facilitate a dominant NH_4^+ absorption route in roots. NO_3^- acquisition in roots is mediated by the transporter genes belonging to both nitrate/peptide transporter family (NPF) and nitrate transporter 2 (NRT2) family (Wang et al., 2018). To date, multiple NO_3^- transporters in rice have been well characterized (see the review by Fan et al., 2017; Tang et al., 2019; Wang et al., 2020). Among them, OsNRT2.4 (named as NRT2.4 in this article) has been characterized as a dual-affinity NO_3^- transporter and functions in NO_3^--regulated root growth and NO_3^- remobilization in rice (Wei et al., 2018).

The N requirement in plant fluctuates at different developmental stages, and is largely influenced by endogenous growth demand, that is, the sink strength (Pitman and Cram, 1973; Glass, 2003). Plants adjust root architecture and N transporter activity to meet the variable N demand. Nowadays, improving N uptake efficiency (NUpE) in crops is of great importance for the sustainable agricultural practice. It should be noted that NUpE in crop is determined by both N acquisition rate and growth duration (reviewed by Glass, 2003; Garnett et al., 2009; Xu et al., 2012).

Crop yield highly relies on an appropriate growth period to ensure the optimization of the use of light, heat, water, and nutrient resources in agricultural practice. The growth period of grain crops consists of vegetative stage before flowering (heading in rice) and thereafter reproductive stage (Minoli et al., 2019). The time and proportion allocated to vegetative and reproductive growth play critical roles in determining the potential of natural resource capture by crops during the growing season (Sharma, 1992; Egli, 2011). The flowering time that is the transitional state from vegetative to reproductive stage basically determines the entire growth period (Egli, 2011; Fischer, 2016). Early transition decreases yield, while delayed transition can lead to larger panicles (Kyozuka et al., 2014). Flowering time is determined by multiple endogenous and exogenous factors to ensure the transition to reproduction with favorable environmental conditions (Song et al., 2013; Cho et al., 2017).

Many floral factors and their associated genetic components for determining flowering time under various environmental conditions have been identified in Arabidopsis (*Arabidopsis thaliana*) and rice (Kazan and Lyons, 2015; Cho et al., 2017; Zhou et al., 2021), while their potential roles in regulating root nutrient acquisition remain unclear. We have previously demonstrated that N-mediated heading date-1 (Nhd1) regulates flowering time via activating transcriptional expression of *Heading date 3a* (*Hd3a*; Zhang et al., 2021). In this study, we show that Nhd1 can directly activate the expression of a high-affinity NH_4^+ transporter gene *OsAMT1;3* (named as *AMT1.3* in this article) and a dual affinity NO_3^- transporter gene *NRT2.4*. Physiological, molecular, and genetic analysis of *nhd1*, *amt1.3*, and *nrt2.4* mutants revealed that root growth and N uptake rate were decreased in *nhd1* mutants resulting from the suppression of *AMT1.3* and *NRT2.4*, while total N accumulation and NUpE of *nhd1* mutants were increased at low N supply due to a prolonged vegetative and entire growth period. Our findings not only extend the Nhd1-centred regulatory pathway of N use efficiency (NUE), but also highlight the critical role of flowering time in maintaining plant NUpE, particularly in paddy field with low N input.

Results

Nhd1 is required for root growth under various N supplies and high-affinity NH_4^+ uptake

To test whether the increased total N accumulation and NUpE of *nhd1* mutants under limited N supply (Zhang et al., 2021) is related to the alteration of root development and/or N absorption capacity, we monitored the root morphology and ^{15}N-labeled N uptake rate of *nhd1* mutants under different N supplies. Compared with wild-type (WT) and a segregated nontransgenic line (designed as a negative control [NC]), *nhd1* mutants showed a decrease in seminal root (SR) length, total lateral root (LR) number, and LR length when low (0.25 mM) NO_3^- (LNi), high (2.5 mM) NO_3^- (HNi), or low (0.25 mM) NH_4^+ (LA) was supplied as the sole N source (Figure 1, A–D). In contrast, in the presence of a high level (2.5 mM) NH_4^+ (HA), no alteration in any of the root traits was observed in the *nhd1* mutants (Figure 1, A–D).

Compared with WT and NC lines, the $^{15}NO_3^-$ influx rate of *nhd1* mutants was unchanged no matter if exposing to LNi or HNi (Figure 1E). In contrast, the $^{15}NH_4^+$ influx rate of *nhd1* lines was significantly lower than WT and NC lines under LA supply (Figure 1E). Notably, the root growth or $^{15}NH_4^+$ influx rate between WT, NC, and *nhd1* lines showed no significant difference at HA supply (Figure 1, A–E). These results suggest that the loss of *Nhd1* function in rice actually restricts root growth and N acquisition in the presence of NO_3^- or LA.

Nhd1 directly activates the expression of *NRT2.4* and *AMT1.3* by binding to their promoters

Plasma membrane-localized NO_3^- and NH_4^+ transporters not only contribute to root N uptake but also modulate root growth responses to different forms and concentrations of N (Fan et al., 2017; Jia and von Wiren, 2020). Since expression level of *Nhd1* was increased with the increase of N concentration in both root and shoot (Supplemental Figure S1A; Zhang et al., 2021), we investigated whether the impaired root growth in *nhd1* mutants were caused by altered expression of N transporter genes. We first examined the expression of six *NPF/NRT2/AMT* genes that contain Nhd1-

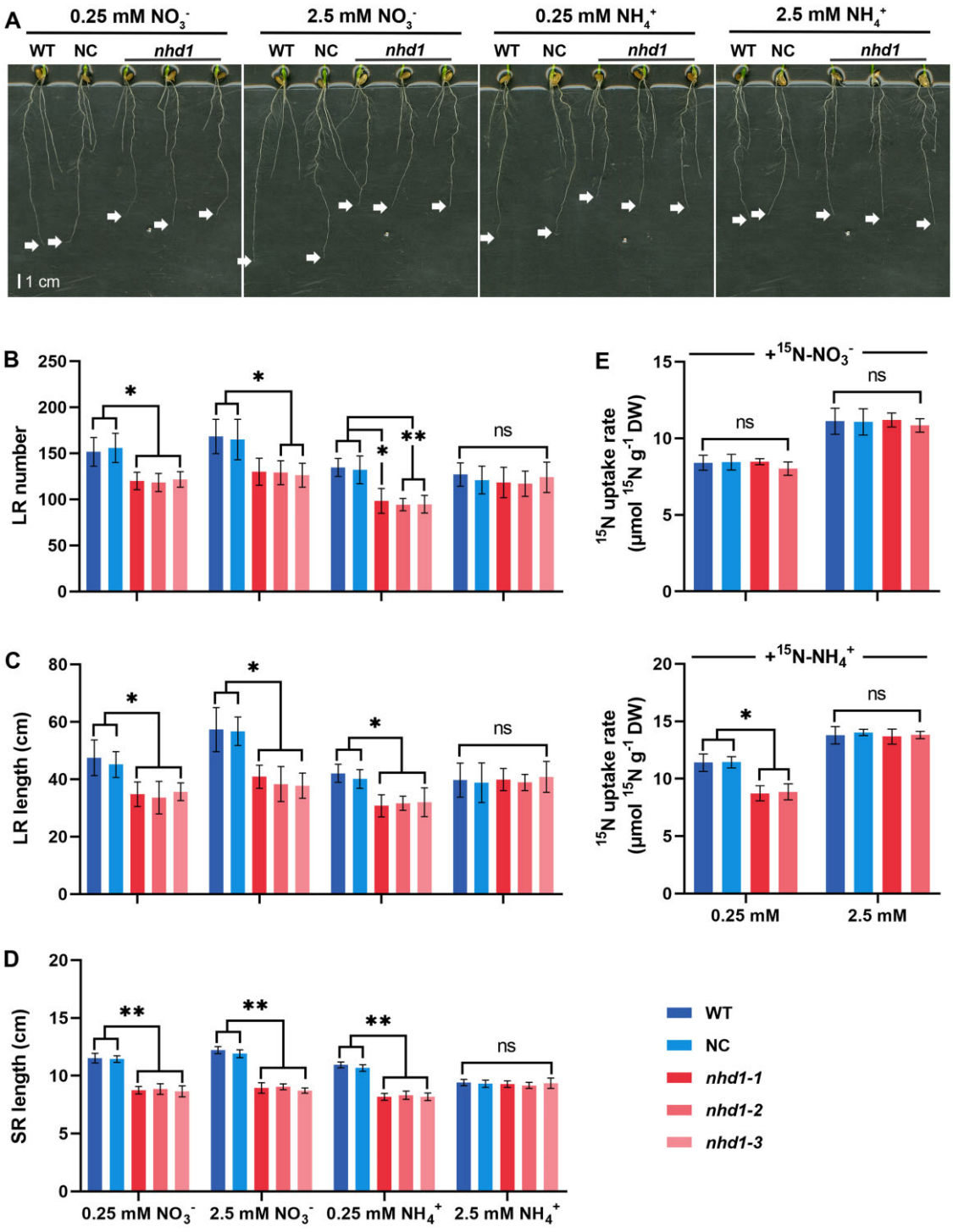

Figure 1 Knockout of *Nhd1* inhibits root growth and reduces $^{15}NH_4^+$ uptake rate under N limited condition. A, Root phenotype of WT (Nip), NC (a segregated nontransgenic line), and *nhd1* mutants. Each line was treated by 0.25 mM and 2.5 mM NO_3^- or NH_4^+ for 7 days. The arrow indicates apical position of the SR. Scale bar, 1 cm. B–D, LR number (B), LR length (C), and SR length (D) of the different lines shown in (A). E, The NO_3^- and NH_4^+ influx rate per root unit weight of WT, NC and *nhd1* mutants supplied with 0.125 mM and 1.25 mM $Ca(^{15}NO_3)_2$ (atom% ^{15}N:$^{15}NO_3^-$, 40%) or $(^{15}NH_4)_2SO_4$ (atom% ^{15}N:$^{15}NH_4^+$, 40%) for 5 min. DW indicates dry weight. Values in (B–E) are means ± SD ($n \geqslant 3$). One-way ANOVA (Analysis of Variance) was used for the statistical analysis (*$P \leqslant 0.05$; **$P \leqslant 0.01$).

binding site (NBS) in their promoter regions (Zhang et al., 2021; Supplemental Figure S1B). Among these genes, only *NRT2.4* and *AMT1.3* expression was dramatically suppressed in both root and shoot of *nhd1* mutants regardless of N concentration (Supplemental Figure S1C; Figure 2, A and G). Notably, the promoters of *NRT2.4* and *AMT1.3* both contain two NBS, the core sequence: AAAAATCT (Figure 2, B and H). In addition, we compared the expression of several

previously reported NO_3^- *assimilation-related protein* (*NRT/NAR*)/*AMT* genes that do not contain NBS in their promoters (Supplemental Figure S1B) in WT and *nhd1* mutants. Loss of Nhd1 function did not affect expression of *NRT1.1a*, *NRT1.1b*, *NRT2.1*, *NRT2.3*, *NAR2.1*, and *AMT1.2* or decreased expression of *AMT1.1* and *AMT2.1* only in shoot, but not in root (Supplemental Figure S1D), suggesting that these transporter genes might be not the direct targets of Nhd1 in rice.

To investigate whether Nhd1 is capable of directly binding to the promoters of *NRT2.4* and *AMT1.3*, we conducted the yeast one-hybrid assay, electrophoretic mobility shift assay (EMSA), chromatin immunoprecipitation (ChIP)-qPCR (quantitative PCR) assay and transactivation assay of LUC (Luciferase)-report driven by *NRT2.4* or *AMT1.3* promoter (Figure 2, C–F and I–K). All these results confirm that Nhd1 can directly bind to NBS-containing fragments of *NRT2.4* and *AMT1.3* promoters to activate their expression.

AMT1.3 or NRT2.4 functions downstream of Nhd1 in facilitating high-affinity NH_4^+ uptake and NO_3^- partitioning, respectively

To investigate the cellular localization of *Nhd1* and *AMT1.3* in rice roots, we performed immunostaining analysis with an antibody against GUS driven by their respective promoter. In crown root, *Nhd1* was expressed in the exodermis, cortex, pericycle, and vascular parenchyma (including the phloem companion cells) but not in the degenerated/exfoliated epidermis or sclerenchyma cell layer (Figure 3, A and B); in LR, *Nhd1* was expressed in exodermis, sclerenchyma, pericycle, and vascular parenchyma cells (Figure 3C). Interestingly, *AMT1.3* was specifically expressed in the phloem companion cells in crown root (Figure 3, D and E). However, *AMT1.3* expression was confined to the sclerenchyma cell layer, pericycle, and vascular parenchyma cells in LR (Figure 3F). In previous studies, *NRT2.4* was found to be expressed in the phloem companion cell in crown root (Wei et al., 2018). Nevertheless, *Nhd1* co-localized with *AMT1.3* in all the cell types showing *AMT1.3* expression.

To investigate whether *AMT1.3* is responsible for Nhd1-dependent regulation of NH_4^+ uptake, the biochemical function and physiological role of *AMT1.3* were characterized. It has previously been reported that *AMT1.3* is induced by N-deficiency in rice roots and is able to complement a yeast mutant line defective in NH_4^+ uptake under LA condition (Sonoda et al., 2003; Li et al., 2006), implying that AMT1.3 serves as a high-affinity NH_4^+ transporter.

In this study, we reinforced this conclusion by examining the transport activity of *AMT1.3* in *Xenopus laevis* oocytes. Bathed with 0.25-mM $^{15}NH_4^+$, *AMT1.3* cRNA-injected oocytes exhibited a one-fold increase of ^{15}N-uptake in comparison to the water-injected control at pH 5.5 or pH 7.4, whereas no significant NH_4^+ uptake activity was detected when oocytes were incubated in 2.5-mM $^{15}NH_4^+$ (Figure 4A). In addition, the K_m value of AMT1.3 for NH_4^+ was estimated to be 63 μM (Figure 4B).

Next, we generated *amt1.3* mutant lines through the CRISPR/Cas9 (Clustered Regularly Interspaced Short Palindromic Repeats associated 9) system (Supplemental Figure S2). Similar to that found in *nhd1* mutants, NH_4^+ uptake was reduced in *amt1.3* mutants when NH_4^+ was supplied at a low concentration (Figure 4C). This result indicated that the suppressed expression of *AMT1.3* in *nhd1* mutant may be the cause of the impaired NH_4^+ uptake. To verify the potential genetic interaction between Nhd1 and *AMT1.3*/*NRT2.4*, *AMT1.3* and *NRT2.4* were overexpressed in the *nhd1* mutant background, generating *nhd1/2.4-OE* and *nhd1/1.3-OE* lines (Supplemental Figure S3A). It showed that the overexpression of *AMT1.3* recovered NH_4^+ uptake in *nhd1* mutant to a similar extent as in WT (Figures 1, E and 4, D), confirming that AMT1.3 functions downstream of Nhd1 in facilitating high-affinity NH_4^+ uptake in roots. All these results suggest that Nhd1 is required for maintaining high-affinity NH_4^+ influx via promoting the transcription of *AMT1.3* in rice roots.

In our previous work, we demonstrated that NRT2.4 is a dual affinity NO_3^- transporter and responsible for NO_3^--regulated root development and NO_3^- translocation, but NRT2.4 does not directly mediate NO_3^- absorption in rice roots (Wei et al., 2018). Consistent with this, neither the knockout of *Nhd1* or *NRT2.4* nor the overexpression of *NRT2.4* in *nhd1* mutant altered NO_3^- acquisition in roots (Figures 1, E, 4, C and D), implying that Nhd1–NRT2.4 module does not directly regulate NO_3^- uptake in rice root. Moreover, the mutation of either *Nhd1* or *NRT2.4* resulted in a higher accumulation of $^{15}NO_3^-$ in CS (the mixture of basal nodes and leaf sheaths), and a lower $^{15}NO_3^-$ distribution in leaf blade (Figure 4E). When $^{15}NO_3^-$ was supplied to leaf, the mutation of *Nhd1* and *NRT2.4* resulted in more accumulation of ^{15}N in shoot basal, and decreased ^{15}N accumulation in the youngest leaf blade, while such impaired distribution of NO_3^- in the shoot of *nhd1* mutant could be rescued by overexpression of *NRT2.4* (Figure 4F). The result is in agreement with our previous finding that NRT2.4 contributes to NO_3^- remobilization in shoot (Wei et al., 2018) and further supported the notion that NRT2.4 functions downstream of Nhd1.

NRT2.4 and AMT1.3 are responsible for Nhd1-mediated root growth responses to various N supplies

We wondered whether the defect of root development in *nhd1* mutants was caused by the suppression of *NRT2.4* and *AMT1.3*. Thus, the root traits of *nrt2.4* and *amt1.3* mutant lines together with the WT, NC line, and *nhd1* mutants were examined in a hydroponic system supplied with various N sources. Under NO_3^- supplies (either LNi or HNi conditions), *nrt2.4* mutants showed defective root growth phenotypes like that of *nhd1* mutants, namely decreased SR length, LR number, and LR length, whereas the root growth of *amt1.3* mutants remained unchanged at the same condition (Figure 5, A–D). In the presence of LA supply, *amt1.3* mutants but not *nrt2.4* mutants displayed an impairment in their root traits like that in *nhd1* mutants, while no

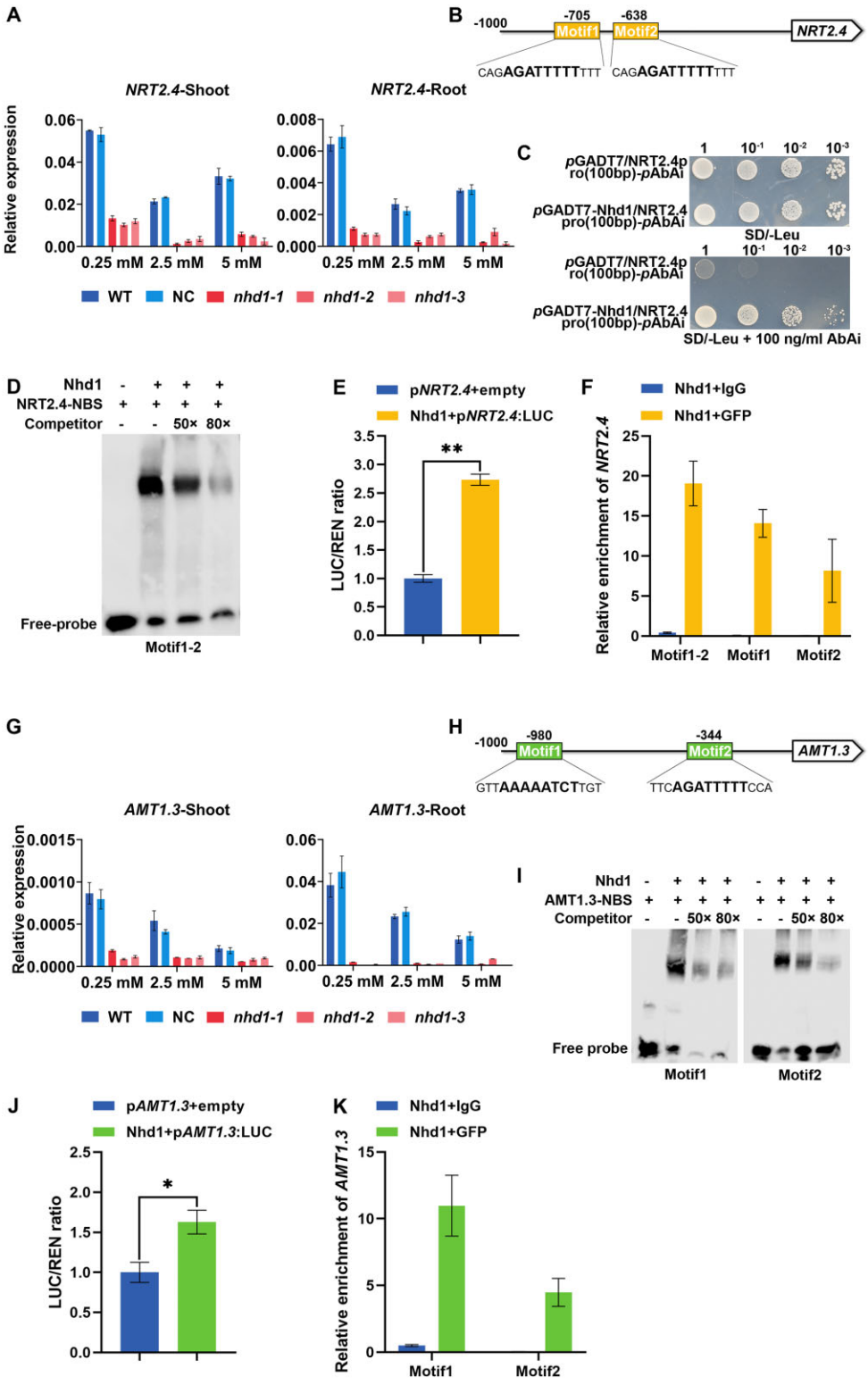

Figure 2 Nhd1 directly binds to NBS in the promoters of *NRT2.4* and *AMT1.3*. A and G, Relative expression levels of *NRT2.4* (A) and *AMT1.3* (G) in the leaves and roots of WT and *nhd1* mutants treated with 0.25, 2.5, and 5 mM N (used NH_4NO_3) quantified by RT-qPCR (Real-time Quantitative PCR). WT (Nip), NC (a segregated nontransgenic line). B and H, Sequence and location of two NBS motifs in the promoter of *NRT2.4* (B) and *AMT1.3* (H). C, Nhd1 binds to the *NRT2.4* promoter region in the yeast-one hybrid system. D and I, EMSA of in vitro Nhd1 binding to the promoter of *NRT2.4* (D) and *AMT1.3* (I). E and J, Transactivation of Nhd1 on the promoter of *NRT2.4* (E) and *AMT1.3* (J) in rice leaf protoplasts. F and K, ChIP-qPCR analysis of Nhd1 binding to the *NRT2.4* (F) and *AMT1.3* (K) promoter region. Values in (A, E, F, G, J, and K) are means ± SD ($n \geqslant 3$). One-way ANOVA was used for the statistical analysis (*$P \leqslant 0.05$; **$P \leqslant 0.01$).

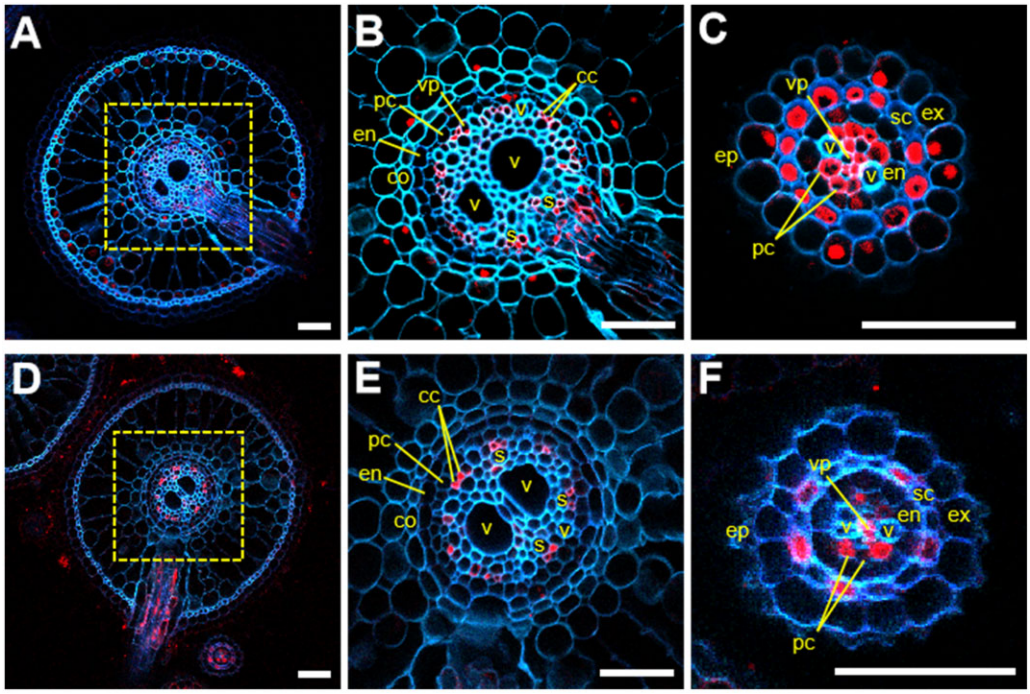

Figure 3 Cellular localization of *Nhd1* and *AMT1.3* in rice roots. A–C, Cellular localization of *Nhd1* in adventitious root (A and B) and LR (C). D–F, Cellular localization of *AMT1.3* in adventitious root (D and E) and LR (F). Immunostaining was performed against the GUS antibody with the transgenic rice plants carrying the *ProNhd1:GUS* and *ProAMT1.3:GUS* constructs. B and E are the magnified views of the regions in the dotted boxes in (A) and (D), respectively. ep, epidermis; ex, exodermis; sc, sclerenchyma; co, cortex; en, endodermis; pc, pericycle; vp, vascular parenchyma; cc, phloem companion cell; v, metaxylem vessel; s, metaphloem sieve tube. Bars, 50 μm.

significant alteration of all root traits was detected among all the genotypes upon HA supply (Figure 5, A–D). These results suggest that the altered root development of *nhd1* mutants under various N supplies is very likely due to the reduced expression of *NRT2.4* and *AMT1.3*, respectively (Figures 1, A–D, 2, A, G, and 5, A–D).

To validate this hypothesis, the root growth responses of *nhd1/2.4-OE* and *nhd1/1.3-OE* plants to various N supplies were further examined by hydroponics. It was shown that the defects of root growth in *nhd1* mutants were largely restored by the overexpression of *NRT2.4* under NO_3^- supplies, or by the overexpression of AMT1.3 under LA and under an even lower level of external NH_4^+ (0.1 mM) (Figure 5, E–G; Supplemental Figure S3, B–F; Supplemental Table S1). Altogether, these results demonstrate that Nhd1 modulates root growth responses to NO_3^- and NH_4^+ via governing the expression of *NRT2.4* and *AMT1.3*, respectively.

Intriguingly, the mutation of *NRT2.4* did not change root growth (Figure 5) and ^{15}N-NH_4^+ absorption rate (Figure 4C) when NH_4^+ was the only N source. In similar, the mutation of *AMT1.3* did not affect the root growth (Figure 5) and distribution of N under varied NO_3^- supplies (Figure 4E). Meanwhile, we detected *AMT1.3* expression in *nrt2.4* mutant and *NRT2.4* expression in *amt1.3* mutant, and no significant change was observed between WT and the mutants (Supplemental Figure S4). These results indicate that even though both *NRT2.4* and *AMT1.3* function downstream of Nhd1, they regulate root response to NO_3^- and NO_3^- distribution, and high-affinity NH_4^+ acquisition independently.

Nhd1, AMT1.3, and NRT2.4 are involved in maintaining root growth at low N supplied paddy soil

Rice grown in paddy field takes up NH_4^+ as the major form of inorganic N and NO_3^- as an accompanying N source (Arth et al., 1998; Kirk and Kronzucker, 2005; Li et al., 2008; Sun et al., 2016). Following a common agricultural practice, we transplanted 28-day-old seedlings of the knockout lines of *nhd1*, *amt1.3*, and *nrt2.4* together with the WT and NC lines in paddy field applied with 150 or 300 kg N ha^{-1}, and monitored their root traits during the entire growth season.

We sampled the roots from soil at the transplanting, tillering, flowering (heading), and mature grain stage. Since the flowering time and fully grain maturation of *nhd1* mutants were delayed for ~2 weeks in comparison to WT, NC, *amt1.3*, and *nrt2.4* lines due to inactivation of *Nhd1* and floral factor *Hd3a* (Zhang et al., 2021; Supplemental Figure S5, B–E), we performed an additional sampling for *nhd1* mutants at its mature grain stage (105 days after seedling emergence [DAE]). When grown in the paddy field with high N input, no significant difference in either root length or total root dry weight per plant was observed in all the mutant lines compared with WT and NC during the entire growth season (Figure 6, A–C; Supplemental Figures S5A

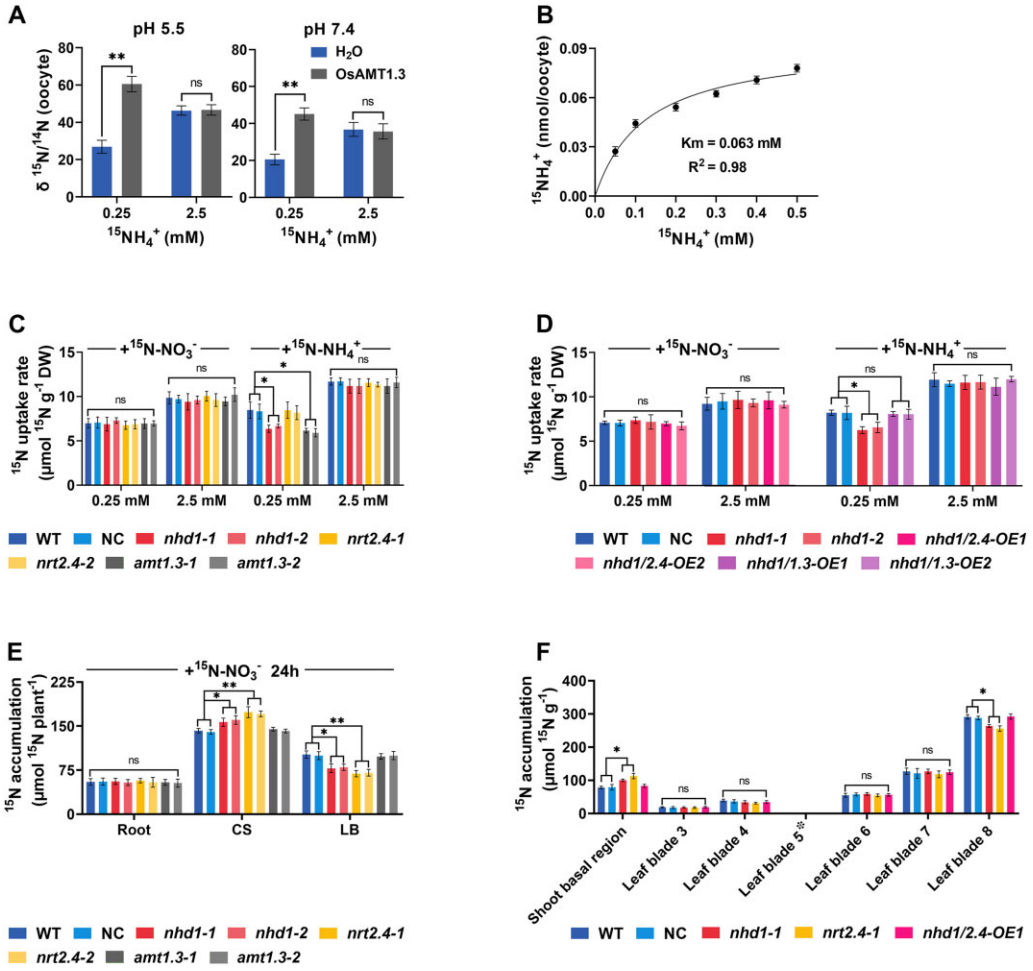

Figure 4 Characterization of AMT1.3 as high-affinity NH_4^+ transporter and distribution of root or leaf acquired $^{15}NO_3^-$ to sink organs of *nhd1* and *nrt2.4* mutants. A, Results of NO_3^- uptake assay in *Xenopus* oocytes injected with *AMT1.3* cRNA using $(^{15}NH_4)_2SO_4$ at pH 5.5 and pH 7.4 medium, respectively. B, NO_3^- uptake kinetics of *AMT1.3* in *Xenopus* oocytes. *AMT1.3* cRNA was injected into oocytes, which were incubated in the ND96 solution containing 0.05, 0.1, 0.2, 0.3, 0.4, and 0.5 mM ^{15}N using $(^{15}NH_4)_2SO_4$ for 2 h at pH 5.5. C, The ^{15}N uptake rate per root unit weight of WT, NC, *nhd1*, *nrt2.4*, and *amt1.3* mutants supplied with 0.25 mM and 2.5 mM N (used $Ca(^{15}NO_3)_2$ or $(^{15}NH_4)_2SO_4$) for 5 min. D, The ^{15}N uptake rate in roots of WT, NC, *nhd1*, *nhd1/2.4-OE*, and *nhd1/1.3-OE* under 0.25 mM and 2.5 mM N (used $Ca(^{15}NO_3)_2$ or $(^{15}NH_4)_2SO_4$) for 5 min. E, Allocation of root acquired ^{15}N-NO_3^- in the root, culm (basal node) and sheath (CS), and leaf blades (LB) of WT, NC and the mutants of *nhd1*, *amt1.3*, and *nrt2.4*. The plants were supplied with 2.5 mM $Ca(^{15}NO_3)_2$ for 24 h. F, Distribution of ^{15}N-NO_3^- between leaves of WT, NC, and *nhd1*, *nrt2.4*, *nhd1/2.4-OE*. The fifth leaf blade at eight-leaf-old stage was cut at 2 cm from the tip and subsequently exposed to 9 mL of the nutrient solution containing 2.5-mM $Ca(^{15}NO_3)_2$ for 24 h before sampling for the analysis. Asterisks indicating that fifth leaf blade was not used for the measurement. WT (Nip), NC (a segregated nontransgenic line). The values represent means ± SD of five (A and B) and three (C, D, E, and F) biological replicates. One-way ANOVA was used for the statistical analysis (*$P \leqslant 0.05$, **$P \leqslant 0.01$).

and S6; Supplemental Table S2). In contrast, mutations of *Nhd1*, *AMT1.3*, and *NRT2.4* resulted in a dramatic decrease in both root length and total root dry weight when grown in the limited N input paddy field (Figure 6, D–F; Supplemental Figures S5A and S6; Supplemental Table S2).

A mathematical model predicts that NO_3^- accounts for 15%–40% of total N acquired by rice roots cultivated in paddy field (Kirk and Kronzucker, 2005). Therefore, we further conducted a hydroponic experiment mimicking the N availability in paddy soil by providing the plants with a mixture of NO_3^--N and NH_4^+-N at ratio of 1:3 approximately (N1A3) (Mix-LN: 0.06 mM NO_3^- and 0.19 mM NH_4^+; Mix-HN: 0.6 mM NO_3^- and 1.9 mM NH_4^+). As expected, both *nhd1* and *amt1.3* showed suppressed root growth under Mix-LN condition (Figure 6, G–J; Supplemental Table S1). Such a defective root growth of *nhd1* mutants was fully rescued by the overexpression of *AMT1.3* (Figure 6, G–J; Supplemental Table S1), consistent with that shown in Figure 5, E–G and Supplemental Table S1. Surprisingly, unlike the suppressed root growth in hydroponic conditions with NO_3^- as sole N source, *nrt2.4* did not show significant root growth defect under Mix-HN condition (Figure 6, G–J; Supplemental Table S1). Since NH_4^+ is the favorited N form for rice plants (Tabuchi et al., 2007; Xu et al., 2012) and presence of NH_4^+ in growth media largely reduces NO_3^- uptake (Glass, 2003), the constant high ratio of NH_4^+ in

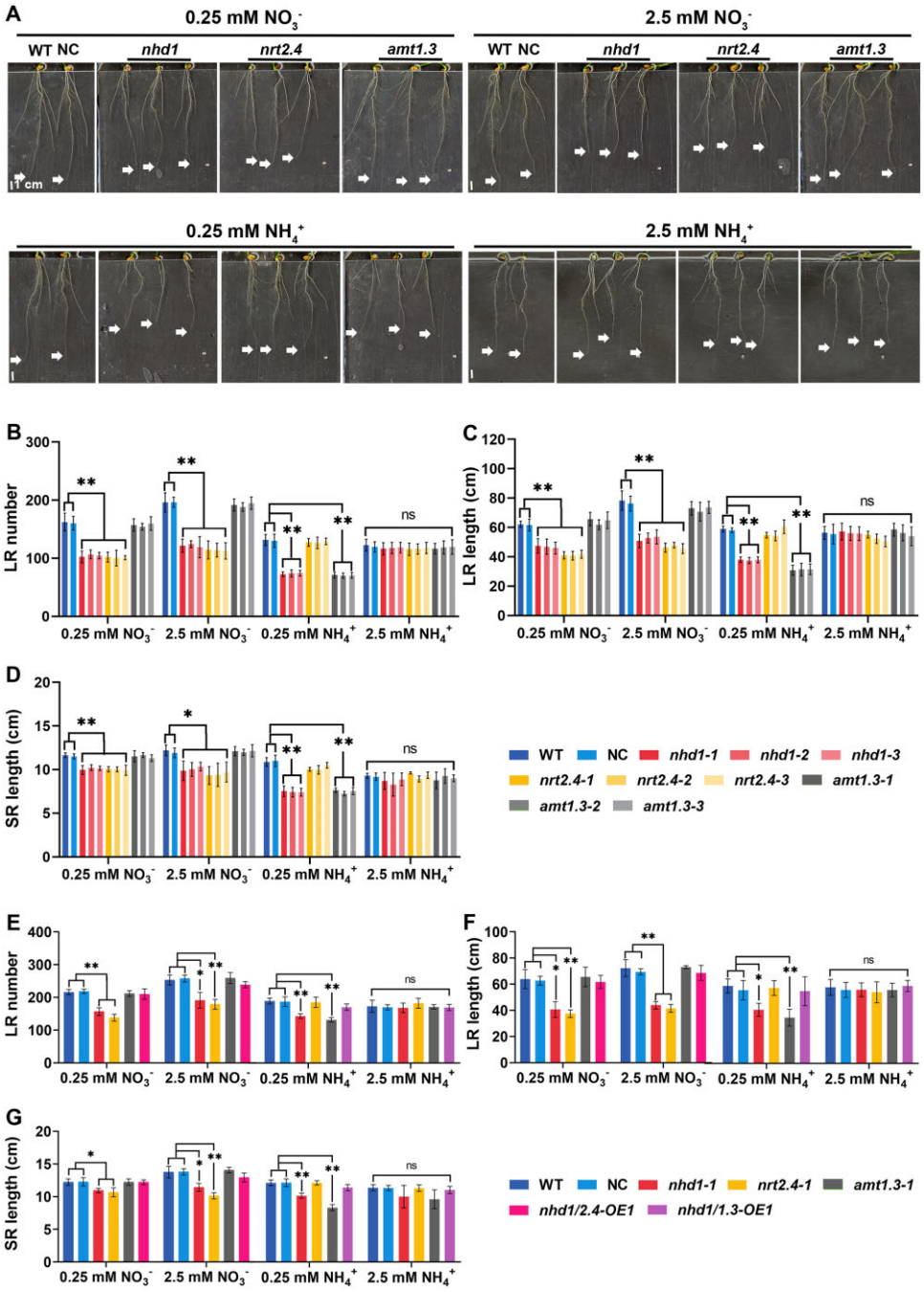

Figure 5 Effects of *Nhd1*, *AMT1.3*, and *NRT2.4* knockout on root growth under various N supplies. A, Root phenotype of WT, NC, and the mutants of *nhd1*, *amt1.3*, and *nrt2.4* under different N treatment for 7 days. The arrow indicates apical position of the SR. Scale bar, 1 cm. B, C, and D, LR number (B), LR length (C), and SR length (D) of the different lines under the treatments shown in (A). E–G, LR number (E), LR length (F), and SR length (G) of WT, NC, the mutants of *nhd1*, *nrt2.4*, *amt1.3*, and *nhd1/2.4-OE*, *nhd1/1.3-OE* under the treatments shown in Supplemental Figure S3B. Raw data are shown in Supplemental Table S1. WT (Nip), NC (a segregated nontransgenic line), LR, SR. Values in (B–G) are means ± SD ($n \geqslant 3$). One-way ANOVA was used for the statistical analysis (*$P \leqslant 0.05$; **$P \leqslant 0.01$).

hydroponics might diminish the root response of *nrt2.4* mutants to NO_3^-. In contrast, due to strong nitrification and rapid root uptake of NH_4^+ (Kirk and Kronzucker, 2005; Tabuchi et al., 2007; Li et al., 2008), the roots might experience relative higher proportion of NO_3^- at the low N supplied paddy soil, thus, led to a strong inhibition of root growth in *nrt2.4* mutants.

Nhd1, AMT1.3, and NRT2.4 function in altering shoot architecture and NUpE in the paddy field

To reveal the function of *Nhd1*, *AMT1.3*, and *NRT2.4* in determining NUpE, we carefully monitored their effect on rice growth and N acquisition in paddy field. In comparison to WT and NC lines, *nhd1* and *nrt2.4* mutants showed a substantial decrease in shoot height and total N accumulation,

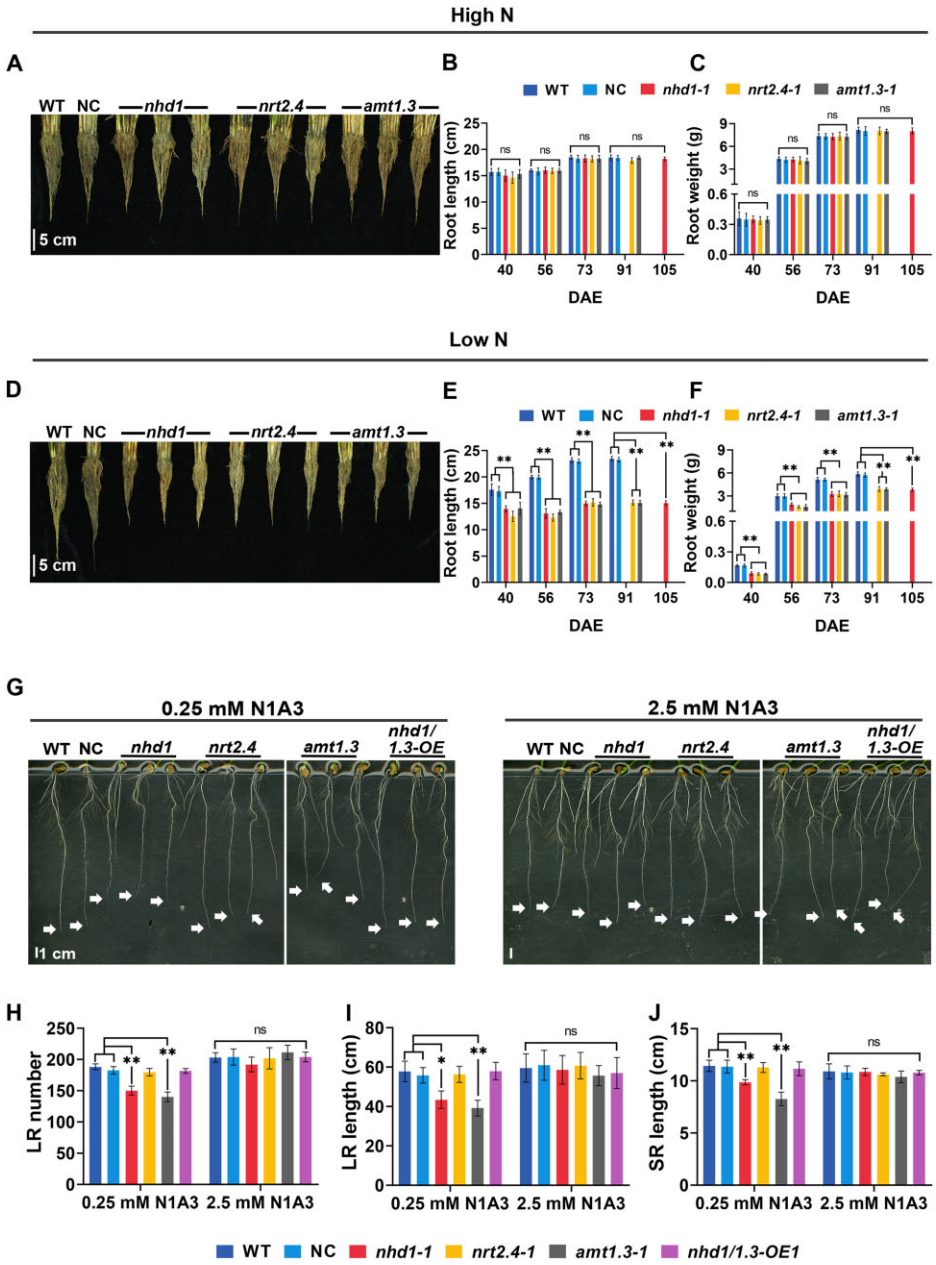

Figure 6 Knockout of *Nhd1*, *NRT2.4*, or *AMT1.3* alters root morphology under N limited soil condition. At 28 DAE (July 14th), the seedlings of WT, NC, and the mutants of *nhd1*, *nrt2.4*, and *amt1.3* were transplanted to the field. A–F, The root distribution, length and weight grown in paddy field until 105 DAE. The mutants of *nhd1* were in the maturity stage, while WT, NC, *nrt2.4*, and *amt1.3* mutants were at 2 weeks after their maturation. High N: 300 kg-N/ha, low N: 150 kg-N/ha. A and D, The roots of the plants after removing of the soil by gentle washing with tap water under high N (A) or low N (D) treatment. Scale bar, 5 cm. B, C, E, and F, Root length and root weight of the plants shown in (A) and (D) and Supplemental Figures S5A and S6 at the different sampling time during entire growth period. Root length was measured from the longest point of the root tip to rhizome junction. Root weight represents the dry weight per plant. The statistical data are shown in Supplemental Table S2. G, Root phenotype of WT, NC, *nhd1*, *nrt2.4*, and *amt1.3* mutants, the complementation line of *nhd1* overexpressing AMT1.3 (*nhd1/1.3-OE*) after the treatments for 7 days. N1A3 (NO_3^-:NH_4^+ = 1:3, mimic the proportion of N forms in the paddy field). The arrow indicates apical position of the SR. Scale bar, 1 cm. H–J, LR number (H), LR length (I), and SR length (J) of plants shown in (G). Raw data of (H–J) are shown in Supplemental Table S1. WT (Nip), NC (a segregated nontransgenic line), LR, and SR. Values in (B, C, E, F, H, I, and J) are means ± SD ($n \geqslant 3$). One-way ANOVA was used for the statistical analysis (*$P \leqslant 0.05$; **$P \leqslant 0.01$).

but more tiller numbers at 56–91 days after emergence irrespective of N supplies (Figure 7, A–E; Supplemental Table S3). Given that NRT2.4 mainly contributes to NO_3^- translocation among rice aerial part (Wei et al., 2018), it makes sense to observe an altered shoot architecture and total N accumulation in *nrt2.4* mutants. Meanwhile, knockout of *AMT1.3* repressed shoot height and reduced N accumulation in paddy field only under low N supply (Figure 7, A–E;

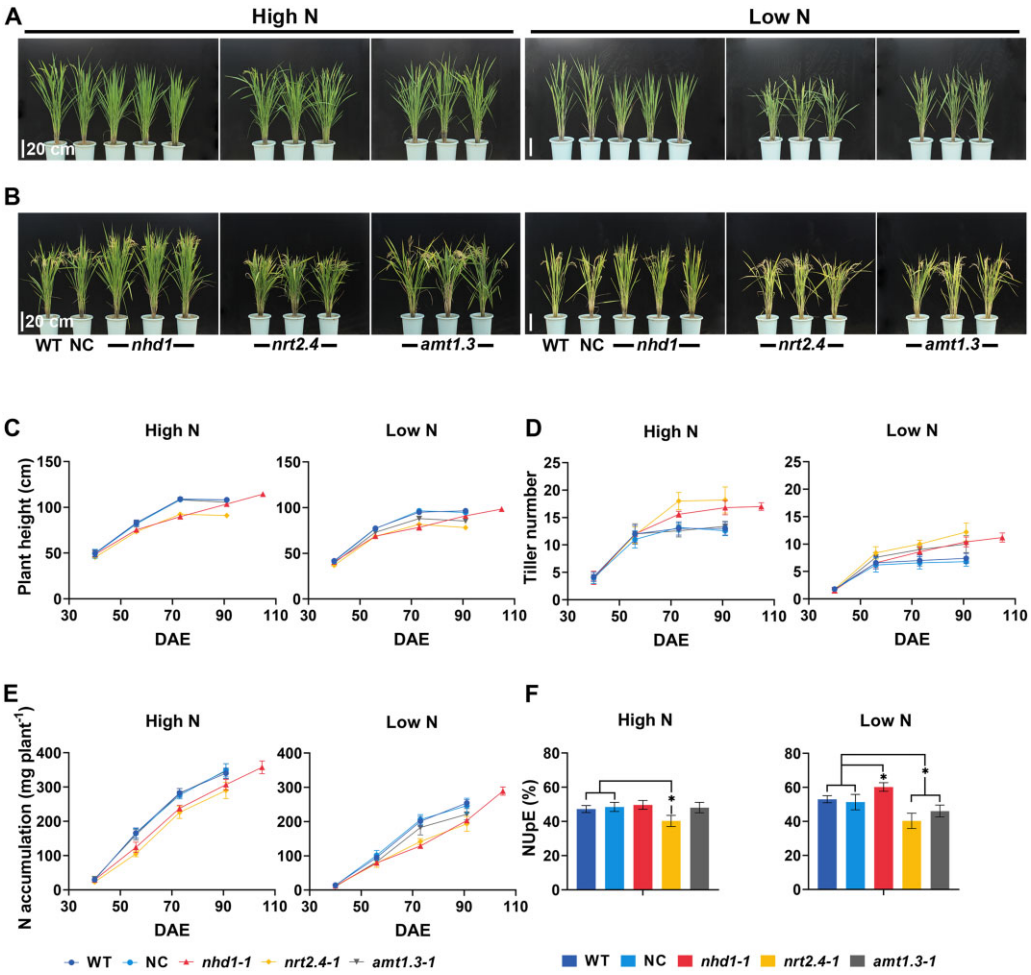

Figure 7 Effects of *Nhd1*, *AMT1.3*, and *NRT2.4* knockout on shoot architecture and N accumulation in paddy field. A–B, The images of the individual representative plant for each line in the paddy field at 73 days (A) and 105 DAE (B). At 73 DAE, WT, NC, *nrt2.4*, and *amt1.3* mutants were at anthesis stage, while *nhd1* mutants were at tillering stage (A). At 105 DAE, the mutants of *nhd1* were at the maturity stage, while WT, NC, *nrt2.4*, *amt1.3* mutants were at 2 weeks after their maturation (B). Scale bar, 20 cm. C–E, The plant height (C), tillering number (D), and total N accumulation per plant (E) during the entire growth stage grown in the paddy field. The mature stage for WT, NC, *nrt2.4*, and *amt1.3* mutants was at 91 DAE, while it was at 105 DAE for *nhd1* mutants. F. The calculated NUpE, the value of total root acquired N divided by total applied fertilizer N at two different N application levels. High N: 300 kg-N/ha, low N: 150 kg-N/ha. WT (Nip), NC (a segregated nontransgenic line). Values in (C, D, E, and F) are means ± SD ($n \geqslant 3$). One-way ANOVA was used for the statistical analysis (*$P \leqslant 0.05$). Raw data of (C–F) are shown in Supplemental Table S3.

Supplemental Table S3), further confirming that AMT1.3 plays a major role in N acquisition as a high-affinity NH_4^+ transporter in rice.

As previously reported, knockout of *Nhd1* substantially limited growth rate resulting in 2-week delay of flowering time (Figure 7A; Supplemental Figure S5, B–C; Zhang et al., 2021). Thereby, prolonged growth period and increased N absorption period of *nhd1* allowed the mutants to accumulate more total N than WT and NC lines at the mature grain stage under low N input condition, leading to an even higher NUpE (Figure 7, E and F; Supplemental Table S3). In contrast, the total N accumulation and NUpE showed no difference with WT under high N input condition (Figure 7, E and F; Supplemental Table S3), indicating that Nhd1–AMT1.3 module plays a minor role in N acquisition in an N-replete environment. In addition, *Nhd1* mutation led to an increase in grain yield under low N condition, while *NRT2.4* mutation led to a decrease in grain yield (Supplemental Figure S7). There was no significant difference in grain yield between *amt1.3* mutants and WT (Supplemental Figure S7).

To further prove the genetic evidence of Nhd1–NRT2.4/AMT1.3 module in rice, we quantified the compensatory effect of *NRT2.4* or *AMT1.3* expression on impaired N accumulation of *nhd1* mutant in paddy field. Overexpression of *NRT2.4* was found to increase N accumulation and NUpE of *nhd1* at both N levels, whereas overexpression of *AMT1.3* increased N accumulation and NUpE of *nhd1* only at N limited condition (Supplemental Figure S8; Supplemental Table S4), which is consistent with short-term results obtained in hydroponic experiments (Figure 4, D and F). It should be noted that knockout of *NRT2.4* and *AMT1.3* or

overexpression of *NRT2.4* and *AMT1.3* in *nhd1* did not significantly alter the flowering and mature time (Supplemental Figure S5, B–E). Inactivation of either *NRT2.4* or *AMT1.3* did not significant affect expression of *Hd3a*, a key florigen gene in rice (Supplemental Figure S5F). The data indicate that NRT2.4 and AMT1.3 are not directly involved in regulating the growth and developmental stages.

Taken together, all the investigations from both hydroponics in the seedling stage and field experiment for entire growth period demonstrate that Nhd1 regulates root development and NH_4^+ uptake capacity by transcriptionally governing *AMT1.3* and *NRT2.4* expression, while knockout of *Nhd1* extends rice growth period and eventually causes an increase of NUpE in a limited N input condition (Figure 8).

Discussion

The altered N accumulation in *nhd1* mutants grown in paddy field results from delayed flowering time and prolonged growth duration

The plant capacity to acquire soil N for maximizing NUpE depends on N demand which is closely related to growth rate and duration (Pitman and Cram, 1973; Glass, 2003). N supply status including forms and concentrations has a great and rapid influence on root and shoot growth rate and developmental stage (Xu et al., 2012; Lin and Tsay, 2017; Jia and von Wiren, 2020). In this study, we found that in addition to the regulation of N-mediated flowering time (Zhang et al., 2021), the transcription factor Nhd1 also controls root growth and N uptake under various N supplies by activating *AMT1.3* and *NRT2.4* expression (Figures 4 and 5). Given that *NRT2.4* or *AMT1.3* mutation did not change flowering time (Supplemental Figure S5, B–E) and expression of floral factor *Hd3a* (Supplemental Figure S5F), it seems that Nhd1 regulation of root growth and N uptake was independent of regulating flowering time. The Nhd1 inactivation resulted in decreased daily root N acquisition irrespective of the N supply levels but increased total N accumulation per plant (NUpE) due to extended growth duration in N limited soil (Figure 8; Supplemental Figure S8).

In rice, N absorption rate and amount varies with growth stages. The daily N uptake rate is low at seedling stage and reaches the highest before the heading stage, then decreases as the root activity declines (Guindo et al., 1994; Mishra and Salokhe, 2010; Yu et al., 2013). We also found that the daily N uptake at the reproductive stage was much lower than that at the vegetative stage under both N regimes (Figure 7E). The daily N uptake per plant of WT, *nrt2.4*, and *amt1.3* ranged from 3.92 to 5.65 mg/day in the vegetative stage (40–73 DAE) and at 1.95–3.15 mg/day in the reproductive stage (73–91 DAE) under low N condition, while it ranged from 5.86 to 7.66 mg/day and 3.20 to 3.86 mg/day in the respective stage under high N condition (Supplemental Table S5; Figure 7E). Since the majority of total N is distributed to grains at mature grain stage, our results are consistent with previous reports that most of N in rice grains come from the accumulated N in vegetative organs before the full heading (Hashim et al., 2015).

Remarkably, the *nhd1* mutants grown in low N soil maintained higher root N uptake rate (5.48–6.14 mg/day) at the reproductive stage (91–105 DAE) than that (3.72–3.86 mg/day) in its vegetative stage (40–91 DAE), eventually, its total accumulated N exceeded that in WT, *amt1.3* and *nrt2.4* mutants at their respective mature grain stage (Supplemental Table S5; Figure 7E). The relative higher uptake rate of *nhd1* during the last development stage at low N supply might be due to two possibilities. One is lower N accumulated in vegetative organs of *nhd1* before fully flowering (Figure 7E; Supplemental Table S3), the high sink demand of N for grain

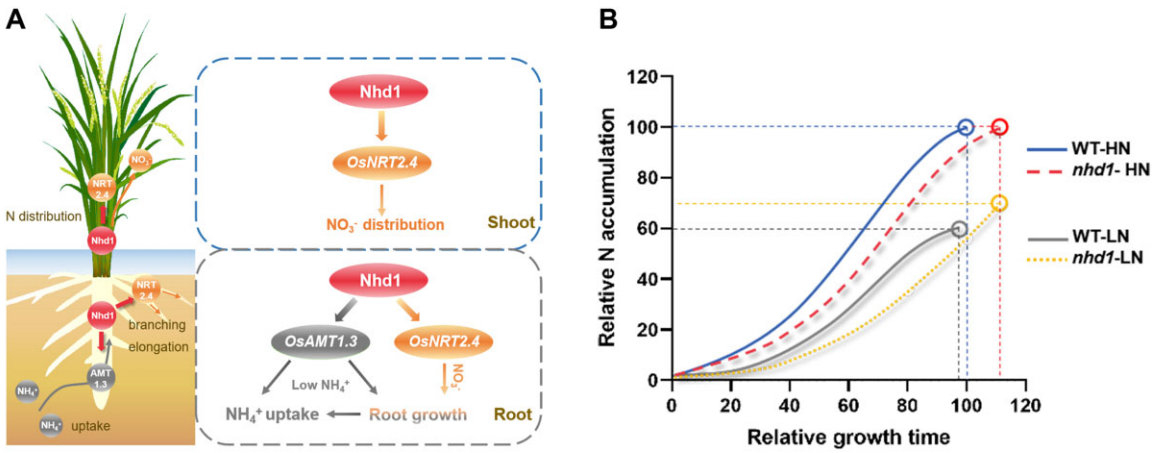

Figure 8 Model of Nhd1-centered regulation of N uptake and utilization efficiency in rice. A, Nhd1 promotes the expression of *AMT1.3* and *NRT2.4* in rice to regulate root growth, high-affinity NH_4^+ uptake rate by AMT1.3 or NO_3^- distribution by NRT2.4 in shoot. Lines ending in arrowheads indicating positive transcriptional activation or increase of root growth, N uptake, or distribution. B, Model of total N accumulation process during the entire growth stage for WT and *nhd1* mutant under high N (HN) or moderate low N (LN) supplies. *X* and *Y* axis units represent relative growth time and relative total N accumulation (percentage of WT under high N treatment). LN supply promotes flowering time and relative earlier maturation for WT, while knockout of *Nhd1* extends flowering time and later maturation irrespective of N supplies (Zhang et al., 2021). The model indicates that plant NUpE is the result of the integration of N uptake rate and growth duration.

development enhances root acquisition of N from soil to compensate for the insufficient N input via re-allocation. The other is less heat stress during its grain filling time for *nhd1* mutants (22°C–27°C at daytime in September) in comparison to WT and other mutant lines (33°C–37°C at daytime in August). The daily optimal average temperature for rice during anthesis and early grain filling stages is 22°C–27°C (Tashiro and Wardlaw, 1991) or 23°C–26°C (Shi et al., 2016), and higher temperature (>33°C–35°C) may repress root activity and N translocation in shoot (Tashiro and Wardlaw, 1991; Cao et al., 2009). Therefore, the optimal temperature in the reproductive stage of *nhd1* mutants might in turn enhance its root N absorption capacity. The results indicate that Nhd1 plays a critical role in balancing N-modulated root and shoot growth, while its influence on extending the vegetative growth stage and plant NUpE largely depends on N availability and environmental condition.

Nhd1 regulates root growth and N uptake rate by promoting the expression of *AMT1.3* and *NRT2.4*

Nhd1 is a light-controlled circadian clock gene that controls flowering time by activating expression of floral regulator *Hd3a* (Zhang et al., 2021). Light signal needs to be promptly recognized by both shoot and root to modulate plant growth and development, however, shoot and root respond differentially to tissue-specific light input (Wang et al., 2021). Nevertheless, we found that knockout of *Nhd1* still largely suppresses root growth both in the hydroponic system (supplied with LA or various levels of NO_3^-; Figure 5, A–D), and paddy field (supplied with low N; Figure 6, D–F). In Arabidopsis, knockout of *CIRCADIAN CLOCK ASSOCIATED 1/LATE ELONGATED HYPOCOTYL* (the putative orthologs of *Nhd1*; Ogiso et al., 2010; Zhang et al., 2021) also inhibited root growth (Yazdanbakhsh et al., 2011). These results suggest that circadian clock regulators may have a conserved role in modulating root growth to adapt to various N supplies.

Plant root growth responses to N supply are regulated by both form and amount of N. Both local and systemic N signals modulate root elongation and branching (Xuan et al., 2017; Jia and von Wiren, 2020). In general, NO_3^- promotes LR elongation, while NH_4^+ stimulates root branching but inhibits root elongation at excessive level (Remans et al., 2006; Lima et al., 2010; Liu et al., 2013; Jia and von Wiren, 2020). In this study, we provided both molecular and genetic evidence revealing that the regulatory module of Nhd1-AMT1.3/NRT2.4 functions in root N uptake and growth response to various N supplies. First, Nhd1 directly binds the NBS in both *AMT1.3* and *NRT2.4* promoters (Figure 2, B–F and H–K), and knockout of *Nhd1* dramatically suppressed their expression in root and shoot (Figure 2, A and G). Second, the SR, LR length, and LR number of *nhd1* mutants were comparable to those of *amt1.3* mutants at LA supply, and to those of *nrt2.4* mutants supplied with either LNi or HNi (Figure 5, A–D). Third, knockout of *Nhd1* decreased ^{15}N-NH_4^+ uptake rate at low concentration range, similar to that found in *amt1.3* mutants (Figure 4C). In addition, a ^{15}N-NO_3^- uptake assay showed that the ^{15}N accumulated in CS (the mixture of basal nodes and sheaths) and leaf blades were increased and decreased, respectively (Figure 4E); meanwhile, the distribution of mature leaf-acquired ^{15}N-NO_3^- to young new leaves was impaired upon mutation of *Nhd1* or *NRT2.4* (Figure 4F). Given that *NRT2.4* is expressed in the phloem of the vascular bundles (VBs) of leaf sheaths and basal nodes (mainly in diffuse VB and to a lesser extent in enlarged VB; Wei et al., 2018) and that *NRT2.4* is a direct target of Nhd1 (Figure 2, A–F), it is very likely that these changes in ^{15}N distribution result from the impaired N remobilization in *nhd1* and *nrt2.4* mutants, consistent with the observation that more N retained in CS and thus less N to leaf blades, especially the young blades that are sink organs and comprise most of the biomass of all the leaf blades, in these two lines (Figure 4E; Wei et al., 2018). Fourth, the defects of *nhd1* mutants in both root growth and N uptake or distribution could be fully rescued by overexpression of *AMT1.3* and *NRT2.4* (Figures 4, D and F and 5, E–G; Supplemental Figure S3, A–F; Supplemental Table S1).

Knockout of *Nhd1* and *NRT2.4* inhibited root growth, but not N absorption rate under various NO_3^- supplies (Figures 4, C and 5, A–D), indicating that the Nhd1–NRT2.4 module may contribute to the root adaption to upland soil where NO_3^- is a dominant N form (Sahrawat and Burford, 1982; D'Andréa et al., 2004; Wang et al., 2019). Interestingly, none of the mutation of *Nhd1*, *AMT1.3*, and *NRT2.4* altered root growth and N uptake rate in high N fertilized paddy field where NH_4^+ accounts for the majority of N sources or in HA supplied hydroponics (Figures 6 and 7, E; Supplemental Tables S2 and S3). The data indicate that some other regulatory pathways govern root N absorption and growth under ammonium-replete condition, which is worth being characterized in the future.

AMT1.3 acts as a high-affinity NH_4^+ transporter for root NH_4^+ acquisition

NH_4^+ can be preferentially taken up by most plants compared with other N forms (Glass, 2003), but excess level of NH_4^+ also causes toxicity in plant cells. Therefore, NH_4^+ uptake and assimilation are tightly controlled. AMT-type NH_4^+ transporters represent the major entry pathways for NH_4^+ uptake in root (Loque and von Wiren, 2004; Tegeder and Masclaux-Daubresse, 2018). In Arabidopsis, four AMTs function in root NH_4^+ acquisition (Loque et al., 2006; Yuan et al., 2007). In NH_4^+-preferred rice plants, OsAMT1.1 has been characterized and shown to be responsible for NH_4^+ uptake and ammonium–potassium homeostasis over LA and HA concentration ranges (Li et al., 2016). However, no NBS in *OsAMT1.1* promoter is presented (Supplemental Figure S1A), suggesting that *OsAMT1.1* is not a direct target of Nhd1.

We detected that *AMT1.3* transcripts are relatively abundant in root and lower in shoot (Figure 2G) with co-localization of *Nhd1* and *AMT1.3* in many cell types of both adventitious and LR (Figure 3, A–F). AMT1.3 functions as a

high-affinity NH_4^+ transporter in oocyte cells (Figure 4, A and B), which is consistent with previous finding that *AMT1.3* can complete yeast NH_4^+ influx at low external NH_4^+ medium (Sonoda et al., 2003). In addition, AMT1.3 functions in root NH_4^+ acquisition only under LA condition (Figure 4C). We noted that Konishi and Ma (2021) recently showed that single knockout of *AMT1.3* did not affect NH_4^+ uptake. This difference in NH_4^+ uptake capacity of *amt1.3* mutants might be due to the differences in the gene mutation sites (Supplemental Figure S2), culture condition, or method for the quantification. We measured ^{15}N-labeled NH_4^+ uptake activity for 5 min at 0.25 mM in roots which is more sensitive than detecting the change of NH_4^+ content in solution with 0.1 mM NH_4^+ as done by Konishi and Ma (2021). Moreover, overexpression of *AMT1.3* can largely restore the impaired NH_4^+ uptake capacity in *nhd1* mutants under LA supply (Figure 4D), further confirming the contribution of AMT1.3 to high-affinity NH_4^+ uptake in rice. Notably, concurrent activation of *AMT1.3* and *OsGOGAT* can increase rice NH_4^+ uptake and remobilization, thus enhancing NUE under N limitation (Lee et al., 2020). Taken together, we conclude that AMT1.3 is a critical transporter for rice to adapt to the limited N supply in paddy field.

Root elongation is commonly inhibited by HA (Figures 1 and 5; Jia and von Wiren, 2020). Intriguingly, a quadruple NH_4^+ transporter mutant (*qko*; *amt1;1 amt1;2 amt1;3 amt2;1*) in Arabidopsis loses the sensitivity to NH_4^+ and shows a decrease of NH_4^+-triggered high-order LR branching (Lima et al., 2010). Given that only AtAMT1;3 can restore the LR proliferation of *qko* mutants, it has been proposed that AtAMT1;3 may act as an NH_4^+ transceptor or mediate a sensing event that occurs downstream of AtAMT1;3 (Duan et al., 2018; Jia and von Wiren, 2020). We found in this study that the defects of root growth in both *amt1.3* and *nhd1* mutants did not correspond to the reduced cumulative uptake of ^{15}N NH_4^+ (Figure 5; Supplemental Figure S3, B–F; Supplemental Table S1). The results indicate that the NH_4^+-dependent root growth response in *amt1.3* and *nhd1* mutants is caused by a sensing event rather than a nutrition effect. Therefore, AMT1.3 may be involved in a yet to be identified regulatory pathway that modulates root development and is independent of NH_4^+ transport process.

In summary, we revealed the crucial roles of the floral regulator Nhd1 in activating *AMT1.3* and *NRT2.4* to modulate root growth, total N acquisition, and NO_3^- distribution, thus finally controlling NUpE, particularly in paddy field with low N availability (Figure 8A). Our findings revealed that both days of N uptake and daily N uptake rate contribute to total N accumulation of plant in a growth season (Figure 8B).

Materials and methods

Plant materials

The Nipponbare (Nip) cultivar of rice (*O. sativa* L. ssp. *japonica*) was used for generating *amt1.3* mutants by CRISPR/Cas9 system. Three homozygous knockout mutants (*amt1.3*) with different mutation sites were identified (Supplemental Figure S2). Mutants of *nrt2.4* and *nhd1* are also Nip background and were generated in previous studies (Wei et al., 2018; Zhang et al., 2021). NC lines were the transgenic segregated lines without mutation in *Nhd1* sequence.

Overexpression of *NRT2.4* (*2.4-OE*) and *AMT1.3* (*1.3-OE*) plants was developed by introducing the full-length cDNA of each gene driven by Cauliflower Mosaic Virus 35S and ubiquitin promoters, respectively, into WT (cv. Nip). The primers used for cloning genes are listed in Supplemental Table S6.

For complementation of possible *AMT1.3* and *NRT2.4* inactivation in *nhd1* mutants, *AMT1.3* and *NRT2.4* overexpression lines were, respectively, crossed with the *nhd1* mutants to generate *nhd1/2.4-OE* and *nhd1/1.3-OE*, their F2 populations were used for the functional assays. Expression of *AMT1.3* and *NRT2.4* in *nhd1/1.3-OE* and *nhd1/2.4-OE* is shown in Supplemental Figure S3A.

Growth conditions for solution culture in phytotron

The seedlings after germination on 1/2 MS (Murashige and Skoog) medium were initially grown in the half-strength IRRI (International Rice Research Institute) nutrient solution (Xia et al., 2015) for 7 days (14-h light/10-h dark photo cycle, day/night temperatures of 30°C/24°C, and relative humidity of ~60%), then transferred to the full IRRI nutrient solution containing 1.25-mM NH_4NO_3 for other 2–3 weeks before the N treatments. The solution was changed every 2 days.

Measurement of root morphology

The seedlings at 5 days after germination with the same bud and root length were selected to ensure the consistency of plant morphology before treatment and transferred to hydroponic media. The IRRI nutrient solution (without N) was changed once a day for 1 week before measurement, NO_3^- and NH_4^+ concentrations in each treatment are given in corresponding figure legend. The root phenotypes were scanned at 600 dpi by using Epson scanner Expression 11000XL. The measurement of LRs and SR were done as described previously (Wei et al., 2018).

In field experiments, the soil was drained 2 days before each observation of root morphology. The soil profile down the root system was dug 30–40 cm in vertical distance from the root–shoot junction of rice and photograph was taken for the representative plant of each line. The deepest root length from the root base was measured as the root length at each growth stage. For getting approximate root biomass, the soil column with $30 \times 30\,cm^2$ area and 40-cm depth surrounded the selected plant was dug out. The clods covered on the roots were removed and the clays stuck on root surface were gently rinsed away by tap water. The roots after removing soils were photographed before were dried to constant weight in oven at 75°C.

RNA extraction, cDNA synthesis, and RT-qPCR

RNA extraction, cDNA synthesis, and RT-qPCR were performed as described in Song et al. (2020). All the primers used for RT-qPCR are listed in Supplemental Table S6.

Yeast one-hybrid assay, EMSA, ChIP assay, and transient transactivation assay of *Nhd1* in rice leaf protoplasts

The binding of Nhd1 to NBS has been verified in previous study (Zhang et al., 2021). The fragments containing NBS in *NRT2.4* or *AMT1.3* promoter were selected for vector construction or direct synthesis of probes used in yeast one-hybrid, EMSA, and ChIP. The specific fragments can be found in Supplemental Table S6. The respective upstream fragment of 2,000-bp DNA of *NRT2.4* or *AMT1.3* translation initiation codon was amplified by PCR from the genomic DNA of Nip cultivar and used for transient transactivation assay. These assays were performed as described by Zhang et al. (2021). The primers for the assays are listed in Supplemental Table S6.

Cloning and cRNA synthesis of *AMT1.3* and NH_4^+ uptake assay in *X. laevis* oocytes

The cDNA of *AMT1.3* was subcloned as a BglII–SpeI fragment into the oocyte expression vector *p*T7Ts (Cleaver et al., 1996) by ClonExpress II One Step Cloning Kit (Vazyme, Nanjing, China). The protocols for oocyte preparation, incubation, and injection were the same as previously described (Feng et al., 2013; Xia et al., 2015). ^{15}N concentration was analyzed by Isotope Ratio Mass Spectrometer system (Flash 2000 HT, Thermo Fisher Scientific, Germany).

Determination of root ^{15}N uptake rate and $^{15}NO_3^-$ distribution

For determination of ^{15}N uptake rate, the seedlings were grown in IRRI nutrient solution for 3 weeks and then N starved for 3 days. The seedlings were first transferred to 0.1-mM $CaSO_4$ for 1 min, then to the IRRI nutrient solution containing 0.25 mM and 2.5 mM $^{15}NH_4^+$ or $^{15}NO_3^-$ for 5 min, and finally to 0.1-mM $CaSO_4$ for 1 min before sampling the roots.

For determination of $^{15}NO_3^-$ distribution in shoot, seedlings were planted in IRRI nutrient solution for 4 weeks, then they were deprived of N for 3 days. After that, these seedlings were transferred into 0.1-mM $CaSO_4$ for 1 min, then to the IRRI nutrient solution containing 5-mM $^{15}NO_3^-$ for 24 h, and finally to 0.1-mM $CaSO_4$ for 1 min before the roots, culm (basal node), and sheaths, and leaf blades were sampled for ^{15}N analysis.

For determination of $^{15}NO_3^-$ redistribution between different leaves, plants at the eight-leaf-old stage were treated with N starved IRRI solution for 3 days, then the fifth leaf blade was cut at 2 cm from the tip with a razor and subsequently exposed to 9 mL of the solution labeled with 2.5-mM $Ca(^{15}NO_3)_2$ for 24 h. After that, shoot basal region and each of the leaf blades from third to eighth (except for fifth) were sampled for ^{15}N analysis.

The samples were placed in an oven at 105°C for 30 min to inactivate the enzymes and transporters (ensuring no further transfer of N after sampling), and further dried to a constant weight at 75°C. The concentration of ^{15}N was analyzed by Isotope Ratio Mass Spectrometer system (Flash 2000 HT, Thermo Fisher Scientific, Germany).

Generation of the transgenic lines of GUS reporter driven by *Nhd1* and *AMT1.3* promoter and immunostaining analysis

The putative promoter of *Nhd1*, upstream fragment of 2,299 bp, and *AMT1.3* promoter, upstream fragment of 2,345-bp DNA of their respective translation initiation codon, were amplified by PCR from the genomic DNA of Nip cultivar. Each promoter was then cloned into the upstream of the *GUSPlus* reporter gene of *p*CAMBIA1300-GM vector (Chang et al., 2019). Transformation of the constructs into Nip and GUS staining followed our previous report (Guo et al., 2020). The primers used for vector construction are listed in Supplemental Table S6. Immunostaining analysis with an antibody against GUS was performed as described in Yamaji and Ma (2007), and sections were observed and photographed by a confocal laser scanning microscope (Leica, Wetzlar, Germany; TCS SP8X). The cell wall autofluorescence was excited with 0.7%–3% ultraviolet light, the collection bandwidth was 410–470 nm, and the gain value was 30%–60%. The collection bandwidth for Alexa Fluor 555 (the secondary antibody) was 560–580 nm, and the gain value was 50%–60%.

Growth conditions and agronomic trait measurement in paddy field

For field experiments, plants were grown in subtropical area, Baima of Nanjing (119°02′E-31°65′ N) at long-day condition with photoperiod of mean 13.5-h daytime and 10.5-h night in summer (in the year 2020 for Figures 6, A–F and 7, A–F; Supplemental Figures S5A and S6, in the year 2021 for Supplemental Figure S8). The paddy soil was derived from yellow-brown earth, its basic properties were pH 6.9, total N 0.63 g/kg, $NaHCO_3$ extractable P 2.7 mg/kg, NH_4OAc extractable K 74 mg/kg.

Total amount of applied N fertilizer was 150 kg/ha (low N) and 300 kg/ha (high N). The N fertilizers (urea and $NH_4H_2PO_4$) was applied at the day before transplanting, tillering/booting, and flowering stage with 50%, 25%, and 25% of total N, respectively. Total 65 kg P/ha ($NH_4H_2PO_4$) and 78 kg K/ha (K_2SO_4) were applied as base fertilizers before transplanting.

For measurement of agronomic traits, five individual plants of each line under low or high N treatment were randomly selected at each stage. The plant height is the length from soil surface to the highest leaf tip, the tiller number indicates the total tillers per plant.

Determination of total N, N uptake rate, and efficiency

Total N in plants were determined by Kjeldahl method and analyzed by continuous flow analyzer (Seal AA3; Li et al., 2006). NUpE,% = [(total acquired N/plant × number of plants/ha) ÷ (total amount of applied fertilizer N/ha)] × 100%. N uptake

rate (mg/day) during vegetative and reproductive stages (Supplemental Table S5) = (net increased N accumulation/plant between the stages) ÷ (days of each stage).

Statistical analysis

Significant differences among the plants or treatments were determined using the IBM SPSS Statistics version 20 program and one-way ANOVA followed by Tukey's test.

Accession numbers

Sequence data from this article can be found in the GenBank/EMBL data libraries under accession numbers: LOC_Os08g06110 (*Nhd1*), LOC_Os01g36720 (*OsNRT2.4*), LOC_Os02g40710 (*OsAMT1;3*), LOC_Os12g44100 (OsNPF2.2), LOC_Os03g48180 (OsNPF2.4), LOC_Os11g12740 (OsNPF4.1), LOC_Os01g54515 (OsNPF4.5), LOC_Os10g33210 (OsNPF5.5), LOC_Os01g65200 (OsNPF5.16), LOC_Os01g01360 (OsNPF6.1), LOC_Os08g05910 (OsNPF6.3), LOC_Os10g40600 (OsNPF6.5), LOC_Os07g41250 (OsNPF7.1), LOC_Os02g47090 (OsNPF7.2), LOC_Os04g50950 (OsNPF7.3), LOC_Os04g50940 (OsNPF7.4), LOC_Os10g42870 (OsNPF7.7), LOC_Os02g46460 (OsNPF7.9), LOC_Os01g04950 (OsNPF8.1), LOC_Os07g01070 (OsNPF8.2), LOC_Os03g51050 (OsNPF8.5), LOC_Os03g13274 (OsNPF8.9), LOC_Os06g49250 (OsNPF8.20),LOC_Os02g38230 (OsNAR2.1), LOC_Os04g40410 (OsNAR2.2), LOC_Os02g02170 (OsNRT2.1), LOC_Os02g02190 (OsNRT2.2), LOC_Os01g50820 (OsNRT2.3), LOC_Os04g43070 (OsAMT1;1), LOC_Os02g40730 (OsAMT1;2), LOC_Os05g39240 (OsAMT2.1), LOC_Os01g61510 (OsAMT2.2), LOC_Os01g61550 (OsAMT2.3), LOC_Os01g65000 (OsAMT3.1), LOC_Os03g62200 (OsAMT3.2), LOC_Os02g34580 (OsAMT3.3), and LOC_Os03g53780 (OsAMT4).

Supplemental data

The following materials are available in the online version of this article.

Supplemental Figure S1. Effect of *Nhd1* knockout on expression of N transporter genes and NBS in their promoters.

Supplemental Figure S2. Schematic diagram of three individual mutations of *AMT1.3* gene generated by CRISPR–Cas9.

Supplemental Figure S3. Overexpression of *NRT2.4* and *AMT1.3* in the *nhd1* mutant restored the root phenotype defects of *nhd1* mutants.

Supplemental Figure S4. Knockout of *NRT2.4* and *AMT1.3* did not affect expression of *AMT1.3* and *NRT2.4*, respectively, in both shoot and root.

Supplemental Figure S5. Effects of *Nhd1*, *NRT2.4*, and *AMT1.3* knockout on root size, days to flowering, and grain maturity in high- or low- N supplied paddy field.

Supplemental Figure S6. Effects of *Nhd1*, *NRT2.4*, and *AMT1.3* knockout on root growth at five different stages in high- or low- N supplied paddy field.

Supplemental Figure S7. Effect of *Nhd1*, *NRT2.4*, and *AMT1.3* knockout on rice grain yield.

Supplemental Figure S8. Effects of *NRT2.4* and *AMT1.3* knockout or overexpression in *nhd1* mutant on shoot architecture and N accumulation in high- or low N supplied paddy field.

Supplemental Table S1. Effects of *NRT2.4* and *AMT1.3* knockout or overexpression in *nhd1* mutant on LR number, length and SR length in hydroponics.

Supplemental Table S2. Effects of *Nhd1*, *NRT2.4*, and *AMT1.3* knockout on length and weight of roots grown in paddy field.

Supplemental Table S3. Effects of *Nhd1*, *NRT2.4*, and *AMT1.3* knockout on shoot architecture and N accumulation of rice grown in paddy field.

Supplemental Table S4. Effects of *NRT2.4* and *AMT1.3* knockout or overexpression in *nhd1* mutant on rice height, tiller number, and N accumulation at different growth stages in paddy field.

Supplemental Table S5. Effects of *Nhd1*, *NRT2.4*, and *AMT1.3* knockout on N uptake rate during vegetative and reproductive stages in paddy field.

Supplemental Table S6. The primer sequences used in this study.

Acknowledgments

We thank Prof. Yan Hua Su (Institute of Soil Science, Chinese Academy of Sciences) for providing the *X. laevis* oocytes. Dr. Cheng Li (Nanjing Agricultural University) for his help in the field experiments.

Funding

This work was supported by National Natural Science Foundation of China (31930101 and 32102474), National Key Research and Development Program of China (2021YFF1000400), Jiangsu Key Research and Development Program (BE2020339), and Jiangsu Natural Science Foundation (BK20210388).

Conflict of interest statement. All authors state no conflict of interest concerning this paper.

References

Andrés F, Coupland G (2012) The genetic basis of flowering responses to seasonal cues. Nat Rev Genet **13**: 627–639

Arth I, Frenzel P, Conrad R (1998) Denitrification coupled to nitrification in the rhizosphere of rice. Soil Biol Biochem **30**: 509–515

Belder P, Bouman BAM, Cabangon R, Guoan L, Quilang EJP, Yuanhua L, Spiertz JHJ, Tuong TP (2004) Effect of water-saving irrigation on rice yield and water use in typical lowland conditions in Asia. Agricl Water Manag **65**: 193–210

Bouman B, Tuong TP (2001) Field water management to save water and increase its productivity in irrigated lowland rice. Agric Water Manag **49**: 11–30

Briones AM Jr Okabe, S Umemiya, Y Ramsing, NB Reichardt, W Okuyama, H (2003) Ammonia-oxidizing bacteria on root biofilms and their possible contribution to N use efficiency of different rice cultivars. Plant Soil **250**: 335–348

Camanes G, Cerezo M, Primo-Millo E, Gojon A, Garcia-Agustin P (2007) Ammonium transport and *CitAMT1* expression are regulated by light and sucrose in Citrus plants. J Exp Bot **58**: 2811–2825

Cao Y, Duan H, Yang L, Wang Z, Liu L, Yang J (2009) Effect of high temperature during heading and early grain filling on grain yield of indica rice cultivars differing in heat-tolerance and its physiological mechanism. Acta Agronomic Sin **35**: 512–521

Chang M, Gu M, Xia Y, Dai X, Dai CR, Zhang J, Wang S, Qu H, Yamaji N, Ma J, Xu GH (2019) OsPHT1;3 mediates uptake, translocation, and remobilization of phosphate under extremely low phosphate regimes. Plant Physiol **179**: 656–670

Chen X, Yao Q, Gao X, Jiang C, Harberd NP, Fu X (2016) Shoot-to-root mobile transcription factor HY5 coordinates plant carbon and nitrogen acquisition. Curr Biol **26**: 640–646

Cho LH, Yoon J, An G (2017) The control of flowering time by environmental factors. Plant J **90**: 708–719

Cleaver OB, Patterson KD, Krieg PA (1996) Overexpression of the tinman-related genes *XNkx-2.5* and *XNkx-2.3* in *Xenopus* embryos results in myocardial hyperplasia. Development **122**: 3549–3556

D'André A, Silva MN, Curi N, Guilherme LG (2004) Carbon and nitrogen storage, and inorganic nitrogen forms in a soil under different management systems. Pesq Agropec Bras **39**: 179–186

Duan F, Giehl RFH, Geldner N, Salt DE, von Wiren N (2018) Root zone-specific localization of AMTs determines ammonium transport pathways and nitrogen allocation to shoots. PLoS Biol **16**: e2006024

Egli DB (2011) Time and the productivity of agronomic crops and cropping systems. Agron J **103**: 743–750

El-Lithy ME, Reymond M, Stich B, Koornneef M, Vreugdenhil D (2010) Relation among plant growth, carbohydrates and flowering time in the *Arabidopsis* Landsberg *erecta* x Kondara recombinant inbred line population. Plant Cell Environ **33**: 1369–1382

Esteban R, Ariz I, Cruz C, Moran JF (2016) Mechanisms of ammonium toxicity and the quest for tolerance. Plant Sci **248**: 92–101

Fan XR, Naz M, Fan XR, Xuan W, Miller AJ, Xu GH (2017) Plant nitrate transporters: from gene function to application. J Exp Bot **68**: 2463–2475

Feng HM, Xia XD, Fan XR, Xu GH, Miller AJ (2013) Optimizing plant transporter expression in Xenopus oocytes. Plant Methods **9**: 48

Feng HM, Yan M, Fan XR, Li BZ, Shen QR, Miller AJ, Xu GH (2011) Spatial expression and regulation of rice high-affinity nitrate transporters by nitrogen and carbon status. J Exp Bot **62**: 2319–2332

Ferreira LM, de Souza VM., Tavares OCH, Zonta E, Santa-Catarina C, de Souza SR, Fernandes MS, Santos LA (2015) *OsAMT1.3* expression alters rice ammonium uptake kinetics and root morphology. Plant Biotechnol Rep **9**: 221–229

Fischer RA (2016) The effect of duration of the vegetative phase in irrigated semi-dwarf spring wheat on phenology, growth and potential yield across sowing dates at low latitude. Field Crop Res **198**: 188–199

Garnett T, Conn V, Kaiser BN (2009) Root based approaches to improving nitrogen use efficiency in plants. Plant Cell Environ **32**: 1272–1283

Gastal F, Lemaire GJ (2002) N uptake and distribution in crops: an agronomical and ecophysiological perspective. J Exp Bot **53**: 789–799

Glass ADM (2003) Nitrogen use efficiency of crop plants: physiological constraints upon nitrogen absorption. Critic Rev Plant Sci **22**: 453–470

Gruber BD, Giehl RF, Friedel S, von Wiren N (2013) Plasticity of the Arabidopsis root system under nutrient deficiencies. Plant Physiol **163**: 161–179

Guindo D, Norman RJ, Wells B (1994) Accumulation of fertilizer nitrogen-15 by rice at different stages of development. Soil Sci Soc Am J **58**: 410–415

Guo N, Hu JQ, Yan M, Qu HY, Luo L, Tegeder M, Xu GH (2020) *Oryza sativa* Lysine-Histidine-type transporter 1 functions in root uptake and root-to-shoot allocation of amino acids in rice. Plant J **103**: 395–411

Gutiérrez RA, Stokes TL, Thum K, Xu X, Obertello M, Katari MS, Tanurdzic M, Dean A, Nero DC, McClung CR et al. (2008) Systems approach identifies an organic nitrogen-responsive gene network that is regulated by the master clock control gene *CCA1*. Proc Natl Acad Sci USA **105**: 4939–4944

Hao D, Zhou J, Yang S, Qi W, Yang K, Su Y (2020) Function and regulation of ammonium transporters in plants. Int J Mol Sci **21**: 3557

Hashim MMa, Yusop MK, Othman R, Wahid SA (2015) Characterization of nitrogen uptake pattern in malaysian rice MR219 at different growth stages using ^{15}N isotope. Rice Sci **22**: 250–254

James AB, Monreal JA, Nimmo GA, Kelly CL, Herzyk P, Jenkins GI, Nimmo HG (2008) The circadian clock in *Arabidopsis* roots is a simplified slave version of the clock in shoots. Science **322**: 1832–1835

Jia Z, von Wiren N (2020) Signaling pathways underlying nitrogen-dependent changes in root system architecture: from model to crop species. J Exp Bot **71**: 4393–4404

Kazan K, Lyons R (2015) The link between flowering time and stress tolerance. J Exp Bot **67**: 47–60

Kirk G, Kronzucker HJ (2005) The potential for nitrification and nitrate uptake in the rhizosphere of wetland plants: a modelling study. Ann Bot **96**: 639–646

Ko D, Helariutta Y (2017) Shoot-root communication in flowering plants. Curr Biol **27**: R973–R978

Konishi N, Ma JF (2021) Three polarly localized ammonium transporter 1 members are cooperatively responsible for ammonium uptake in rice under low ammonium condition. New Phytologist **232**: 1778–1792

Kronzucker H, Glass A, Siddiqi M, Kirk GJ (2000) Comparative kinetic analysis of ammonium and nitrate acquisition by tropical lowland rice: implications for rice cultivation and yield potential. New Phytologist **145**: 471–476.

Kubik-Dobosz G, Bąkiewicz M, Górska A (2001) The importance of root carbohydrate abundance in ammonium uptake. Acta Physiol Plant **23**: 187–192

Kyozuka J, Tokunaga H, Yoshida A (2014) Control of grass inflorescence form by the fine-tuning of meristem phase change. Curr Opin Plant Biol **17**: 110–115

Lee S, Marmagne A, Park J, Fabien C, Yim Y, Kim SJ, Kim TH, Lim PO, Masclaux-Daubresse C, Nam HG (2020) Concurrent activation of *OsAMT1;2* and *OsGOGAT1* in rice leads to enhanced nitrogen use efficiency under nitrogen limitation. Plant J **103**: 7–20

Lei M, Liu Y, Zhang B, Zhao Y, Wang X, Zhou Y, Raghothama KG, Liu D (2011) Genetic and genomic evidence that sucrose is a global regulator of plant responses to phosphate starvation in Arabidopsis. Plant Physiol **156**: 1116–1130

Lejay L, Wirth J, Pervent M, Cross JM, Tillard P, Gojon A (2008) Oxidative pentose phosphate pathway-dependent sugar sensing as a mechanism for regulation of root ion transporters by photosynthesis. Plant Physiol **146**: 2036–2053

Li BZ, Xin WJ, Sun SB, Shen QR, Xu GH (2006) Physiological and molecular responses of nitrogen-starved rice plants to re-supply of different nitrogen sources. Plant Soil **287**: 145–159

Li C, Tang Z, Wei J, Qu HY, Xie Y, Xu GH (2016) The *OsAMT1.1* gene functions in ammonium uptake and ammonium-potassium homeostasis over low and high ammonium concentration ranges. J Genet Genom **43**: 639–649

Li SM, Li BZ, Shi WM (2012) Expression patterns of nine ammonium transporters in rice in response to N status. Pedosphere **22**: 860–869

Li YL, Fan XR, Shen QR (2008) The relationship between rhizosphere nitrification and nitrogen-use efficiency in rice plants. Plant Cell Environ **31**: 73–85

Lima JE, Kojima S, Takahashi H, von Wiren N (2010) Ammonium triggers lateral root branching in *Arabidopsis* in an AMMONIUM TRANSPORTER1;3-dependent manner. Plant Cell **22**: 3621–3633

Lin YL, Tsay YF (2017) Influence of differing nitrate and nitrogen availability on flowering control in Arabidopsis. J Exp Bot **68**: 2603–2609

Liu Y, Lai N, Gao K, Chen F, Yuan L, Mi G (2013) Ammonium inhibits primary root growth by reducing the length of meristem and elongation zone and decreasing elemental expansion rate in the root apex in *Arabidopsis thaliana*. PLoS One **8**: e61031

Loque D, von Wiren N (2004) Regulatory levels for the transport of ammonium in plant roots. J Exp Bot **55**: 1293–1305

Loque D, Yuan L, Kojima S, Gojon A, Wirth J, Gazzarrini S, Ishiyama K, Takahashi H, von Wiren N (2006) Additive contribution of AMT1;1 and AMT1;3 to high-affinity ammonium uptake across the plasma membrane of nitrogen-deficient Arabidopsis roots. Plant J **48**: 522–534

Miller AJ, Cramer MD (2004) Root nitrogen acquisition and assimilation. Plant Soil **274**: 1–36

Minoli S, Egli DB, Rolinski S, Müller C (2019) Modelling cropping periods of grain crops at the global scale. Global Planet Change **174**: 35–46

Mishra A, Salokhe VM (2010) FLOODING STRESS: the effects of planting pattern and water regime on root morphology, physiology and grain yield of rice. J Agron Crop Sci **196**: 368–378

Ogiso E, Takahashi Y, Sasaki T, Yano M, Izawa T (2010) The role of casein kinase II in flowering time regulation has diversified during evolution. Plant Physiol **152**: 808–820

Peng Y, Niu J, Peng Z, Zhang F, Li C (2010) Shoot growth potential drives N uptake in maize plants and correlates with root growth in the soil. Field Crop Res **115**: 85–93

Pitman M, Cram W (1973) Regulation of inorganic ion transport in plants. Ion transport in plants. *In* WP Anderson, ed, Ion Transport in Plants. Elsevier, Amsterdam, Netherlands, pp 465–481

Remans T, Nacry P, Pervent M, Filleur S, Diatloff E, Mounier E, Tillard P, Forde BG, Gojon A (2006) The Arabidopsis NRT1. 1 transporter participates in the signaling pathway triggering root colonization of nitrate-rich patches. Proc Natl Acad Sci USA **103**: 19206–19211

Robledo JM, Medeiros D, Vicente MH, Azevedo AA, Thompson AJ, Peres LEP, Ribeiro DM, Araujo WL, Zsogon A (2020) Control of water-use efficiency by florigen. Plant Cell Environ **43**: 76–86

Sahrawat K, Burford J (1982) Modification of the alkaline permanganate method for assessing the availability of soil nitrogen in upland soils. Soil Sci **133**: 53–57

Sharma RC (1992) Duration of the vegetative and reproductive period in relation to yield performance of spring wheat. Eur J Agron **1**: 133–137

Shi P, Zhu Y, Tang L, Chen J, Sun T, Cao W, Tian Y (2016) Differential effects of temperature and duration of heat stress during anthesis and grain filling stages in rice. Environ Exp Bot **132**: 28–41

Song M, Fan X, Chen J, Qu H, Luo L, Xu G (2020) OsNAR2.1 interaction with OsNIT1 and OsNIT2 functions in root-growth responses to nitrate and ammonium. Plant Physiol **183**: 289–303

Song YH, Ito S, Imaizumi T (2013) Flowering time regulation: photoperiod- and temperature-sensing in leaves. Trend Plant Sci **18**: 575–583

Sonoda Y, Ikeda A, Saiki S, Wirén NV, Yamaya T, Yamaguchi J (2003) Distinct expression and function of three ammonium transporter genes (OsAMT1;1–1;3) in rice. Plant Cell Physiol **44**: 726–734

Sun L, Lu Y, Yu F, Kronzucker HJ, Shi W (2016) Biological nitrification inhibition by rice root exudates and its relationship with nitrogen-use efficiency. New Phytologist **212**: 646–656

Tabuchi M, Abiko T, Yamaya T (2007) Assimilation of ammonium ions and reutilization of nitrogen in rice (*Oryza sativa* L.). J Exp Bot **58**: 2319–2327

Tang W, Ye J, Yao X, Zhao P, Xuan W, Tian Y, Zhang Y, Xu S, An H, Chen G, et al. (2019) Genome-wide associated study identifies NAC42-activated nitrate transporter conferring high nitrogen use efficiency in rice. Nat Commun **10**: 5279

Tang Z, Fan XR, Li Q, Feng HM, Miller AJ, Shen QR, Xu GH (2012) Knockdown of a rice stelar nitrate transporter alters long-distance translocation but not root influx. Plant Physiol **160**: 2052–2063

Tashiro T, Wardlaw I (1991) The effect of high temperature on the accumulation of dry matter, carbon and nitrogen in the kernel of rice. Funct Plant Biol **18**: 259–265

Tegeder M, Masclaux-Daubresse C (2018) Source and sink mechanisms of nitrogen transport and use. New Phytologist **217**: 35–53

Upadhyaya NM, Surin B, Ramm K, Gaudron J, Schünmann PH, Taylor W, Waterhouse PM, Wang MB (2000) *Agrobacterium*-mediated transformation of Australian rice cultivars Jarrah and Amaroo using modified promoters and selectable markers. Funct Plant Biol **27**: 201–210

Wang L, Zhou A, Li J, Yang M, Bu F, Ge L, Chen L, Huang W (2021) Circadian rhythms driving a fast-paced root clock implicate species-specific regulation in *Medicago truncatula*. J Integr Plant Biol **63**: 1537–1554

Wang MY, Siddiqi MY, Ruth TJ, Glass A (1993) Ammonium uptake by rice roots. Plant Physiol **103**: 1249–1258

Wang P, Yamaji N, Inoue K, Mochida K, Ma JF (2019) Plastic transport systems of rice for mineral elements in response to diverse soil environmental changes. New Phytologist **226**: 156–169

Wang S, Chen A, Xie K, Yang X, Luo Z, Chen J, Zeng D, Ren Y, Yang C, Wang L, et al. (2020) Functional analysis of the OsNPF4.5 nitrate transporter reveals a conserved mycorrhizal pathway of nitrogen acquisition in plants. Proc Natl Acad Sci **117**: 16649–16659

Wang YY, Cheng YH, Chen KE, Tsay YF (2018) Nitrate transport, signaling, and use efficiency. Ann Rev Plant Biol **69**: 85–122

Weber K, Burow M (2018) Nitrogen - essential macronutrient and signal controlling flowering time. Physiol Plant **162**: 251–260

Wei J, Zheng Y, Feng H, Qu H, Fan X, Yamaji N, Ma JF, Xu G (2018) OsNRT2.4 encodes a dual-affinity nitrate transporter and functions in nitrate-regulated root growth and nitrate distribution in rice. J Exp Bot **69**: 1095–1107

Xia XD, Fan XR, Wei J, Feng HM, Qu HY, Xie D, Miller AJ, Xu GH (2015) Rice nitrate transporter OsNPF2.4 functions in low-affinity acquisition and long-distance transport. J Exp Bot **66**: 317–331

Xu GH, Fan XR, Miller AJ (2012) Plant nitrogen assimilation and use efficiency. Ann Rev Plant Biol **63**: 153–182

Xuan W, Beeckman T, Xu GH (2017) Plant nitrogen nutrition: sensing and signaling. Curr Opin Plant Biol **39**: 57–65

Yamaji N, Ma J (2007) Spatial distribution and temporal variation of the rice silicon transporter Lsi1. Plant Physiol **143**: 1306–1313

Yazdanbakhsh N, Sulpice R, Graf A, Stitt M, Fisahn J (2011) Circadian control of root elongation and C partitioning in *Arabidopsis thaliana*. Plant Cell Environ **34**: 877–894

Ye T, Li Y, Zhang J, Hou W, Zhou W, Lu J, Xing Y, Li X (2019) Nitrogen, phosphorus, and potassium fertilization affects the flowering time of rice (*Oryza sativa* L.). Glob Ecol Conserv **20**: e00753

YuQG Ye J, Yang SN, Fu JR, Ma JW, Sun WC, Jiang LN, Wang Q, Wang JM (2013) Effects of nitrogen application level on rice nutrient uptake and ammonia volatilization. Rice Sci **20**: 139–147

Yuan L, Loque D, Kojima S, Rauch S, Ishiyama K, Inoue E, Takahashi H, von Wiren N (2007) The organization of high-affinity ammonium uptake in *Arabidopsis* roots depends on the spatial arrangement and biochemical properties of AMT1-type transporters. Plant Cell **19**: 2636–2652

Zhang SN, Zhang YY, Li KN, Yan M, Zhang JF, Yu M, Tang S, Wang LY, Qu HY, Luo L, et al. (2021) Nitrogen mediates flowering time and nitrogen use efficiency via floral regulators in rice. Curr Biol **31**: 671–683

Zhou S, Zhu S, Cui S, Hou H, Wu H, Hao B, Cai L, Xu Z, Liu L, Jiang L, et al. (2021) Transcriptional and post-transcriptional regulation of heading date in rice. New Phytologist **230**: 943–956